DEEP LEVEL TRANSIENT SPECTROSCOPY

OF

MAGNESIUM DOPED INDIUM PHOSPHIDE

Hemavathy Cholan

B.S. College of Engineering, Anna University.
Madras,India, 1983

A thesis submitted to the faculty of the Oregon Graduate Center in partial fulfillment of the requirements for the degree

Master of Science

in

Electrical Engineering

December, 1987

The thesis "Deep Level Transient Spectroscopy of Magnesium Doped Indium Phosphide" by Hemavathy Cholan has been examined and approved by the following Examination Committee:

Dr. Wallace B. Leigh, Assistant Professor

Dr. Russell E. Kremer, Associate Professor

Dr. Raj Solanki, Associate Professor

Dr. Kun Kul Ryoo
Wacker Siltronic Corporation

ACKNOWLEDGEMENTS

I am greatly indebted to Dr. Wallace B. Leigh for his guidance and encouragement in the course of this work. Without his help, this work would not have been completed.

I am also grateful to Dr. Russell E. Kremer, Dr. Raj Solanki and Dr. Kun Kul Ryoo for reviewing this thesis in a relatively short time.

Special thanks are also due to George Howard, Dr. Fred R. Bacher and Dr. Tae Il Oh for growing the InP epilayers used in this work.

Finally I express my gratitude to my husband Cholan, for his support and encouragement.

TABLE OF CONTENTS

LIST OF FIGURES

LIST OF TABLES

ABSTRACT

The deep level characterization of magnesium doped indium phosphide grown by organometallic vapor phase epitaxy (OMVPE) is reported. The chief motive for this work has been the applications of p-InP in optoelectronic and microwave devices. Secondly, very little use has been made of magnesium as a p-type dopant. The properties such as low diffusivity and high solubility in III-V compounds,make magnesium an attractive dopant. However, the high concentrations of Mg used in many device applications cause concern of magnesium-related deep traps being formed and affecting the device performance. Deep level transient spectroscopy (DLTS) was used to characterize deep traps present in InP:Mg samples.

The theory of DLTS is discussed in detail. This method offers direct information about a host of trap parameters such as activation energy, capture cross section, concentration and the nature of the trap. This technique is capable of detecting defects having concentrations as low as ~$10^{12}cm^{-3}$ and is thus sensitive to trap concentrations on the 10 parts per billion scale. However, it does not provide information on the physical identity of

the trap.

CV and IV measurements are made on the Au-InP Schottky diodes. The net acceptor concentration barrier height and ideality factor of the diode are determined from these measurements. The relative values of these characterization methods are discussed.

DLTS measurements over a temperature range of 77^0K - 400^0K revealed the presence of hole traps in InP:Mg samples. A total of three hole traps are observed having activation energies of 0.31, 0.54 and 1.16 eV from the valence band. The capture cross sections are $3.2x10^{-17}$, $1.5x10^{-14}$ and $2.7x10^{-7}$ cm^2 respectively. The concentration of these traps are found to be in the range of 10^{12}-$10^{15}cm^{-3}$.

The physical identity of the traps are merely speculated, as accurate identification requires a much more detailed study which is beyond the scope of this work. Trap H(0.31) is observed in the majority of the samples and is attributed to Mg related complex, while traps H(0.54) and H(1.16) are seen only once and are thought to be some contaminants incorporated during the growth.

CHAPTER - 1

INTRODUCTION

InP and its alloys have received increased attention in recent years owing to their applications in microwave devices, light emitting diodes, heterostructure lasers, photodiodes, photocathodes and solar cells. InP has also become an important substrate material for the growth of GaInAs and GaInAsP. Due to the need for high purity InP for these applications, research in defect analysis has grown considerably. Knowledge of the nature of deep defects has become extremly important as they cause limitations in the performance and reliability of devices. A number of methods have been used in the literature to study deep defects, but one of the most sensitive and successful techniques to-date is deep level transient spectroscopy (DLTS) (1). This method has been used in the present study to characterize Mg-doped InP grown by organo metallic vapor phase epitaxy (OMVPE).

When a wide bandgap semiconductor such as InP is deliberately doped with a large amount of impurity, sometimes deep states will form in the forbidden gap of the

semiconductor. Deep levels that are related to shallow impurities have concentrations that increase as the doping level increases. Thus, they are a particular problem for applications where heavily doped material is needed. An example of such a defect is the DX center in $Al_xGa_{1-x}As$ (2,3). The "D" stands for a shallow donor impurity, which is believed to be paired with an unknown "X" defect. This defect is responsible for many detrimental effects in donor-doped AlGaAs devices. Concern exists that similar levels may exist in other compound semiconductors.

This work involves the DLTS investigation of low to medium doped InP:Mg. This is done because heavily doped material cannot be characterized directly using DLTS, as the sensitivity of the system decreases as doping increases. At the same time, high quality, heavily doped P-type InP is essential for applications such as photocathodes, LEDs, solar cells, etc.

Before proceeding further, it would be appropriate to mention a few properties of InP. InP has a direct bandgap (E_g) of 1.35eV (300°K) and 1.42 eV (0°K). The temperature dependence of the bandgap is given by (4),

$$E_g = [1.421 - 6.63 \times 10^{-4} T^2] / [T+162]$$

It crystallizes in the zincblende structure. Fig.(1) shows the band structure of InP. A detailed discussion of the properties of InP is given in reference (4).

The properties such as high peak velocity, threshold field and thermal conductivity make InP an attractive material for device applications. InP metal semiconductor field effect transistors (MESFETs), for instance, have higher current-gain and cut-off frequency than GaAs devices of equivalent geometry (5). Similarly, InP metal insulator semiconductor field effect transistors (MISFETs) are superior to those made in GaAs, in that the InP/oxide system has lower interface state density and hence is preferable for application requiring low as well as high frequency operation (6). In general, InP FETs are found to be favorable for high power applications as these devices can be operated at higher biases, taking full advantage of the large peak velocity (7).

Yet another application of InP is in the fabrication of the GaInAsP-InP double heterojunction light emitting diodes (LEDs) (8). These are considered to be very promising light sources for fiber optical communications in the 1 - 1.7μm wavelength region. They also provide a better data transmission capacity than the ternary GaAs-AlGaAs

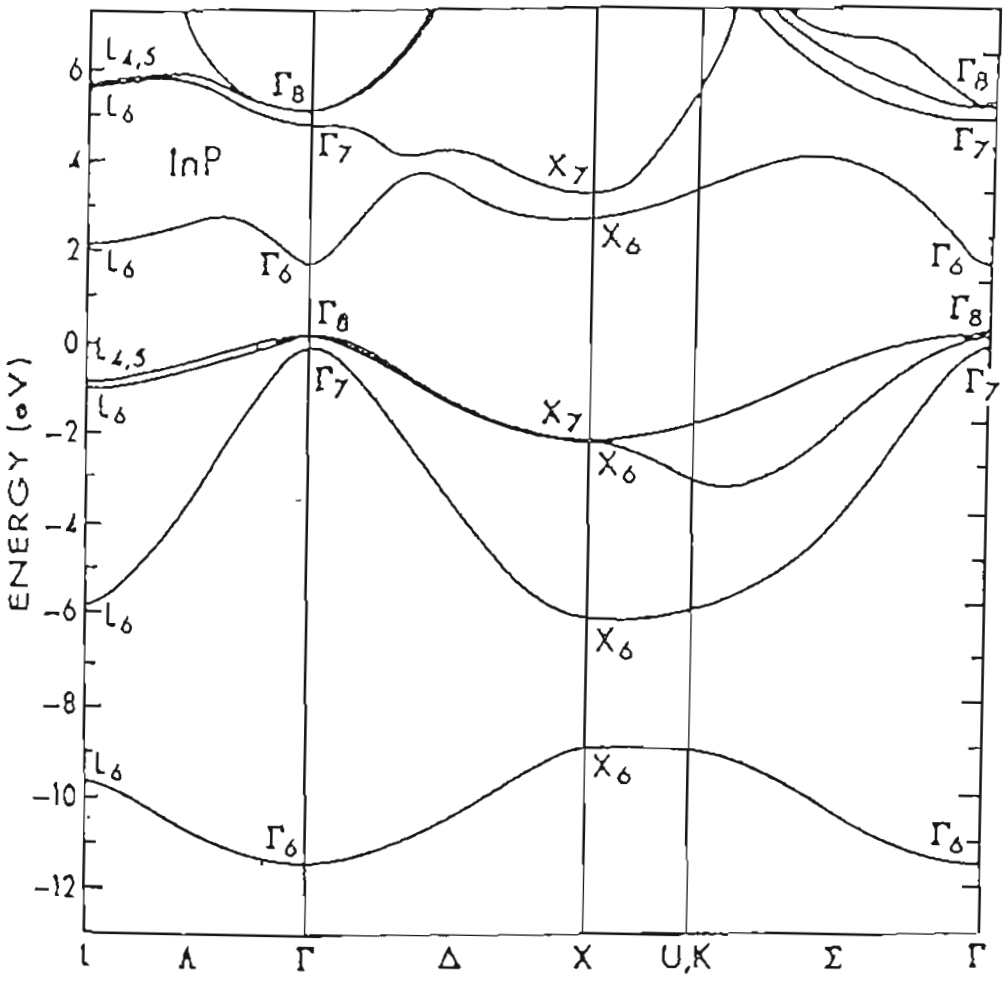

FIG. 1. Band structure of InP.

LEDs.

The double heterostructure laser, fabricated using GaInAsP - InP has low optical loss and minimum material dispersion around 1 - 1.3μm wavelength region. Hence it has applications in high purity silica fiber transmission lines (9).

One of the most important applications of InP, is in the heterojunction photocathodes used in optical detectors (10). The InGaAs / InP heterojunction photocathodes have higher quantum efficiency than the conventional negative affinity photocathodes. The device applications are reviewed in detail in (4).

Most of the above mentioned devices require P - type epitaxial layers of InP, GaInAs and / or GaInAsP. Emission devices such as light emitting diodes and solid state lasers require heavily doped P - type material to ensure recombination is maintained in the active region. Heavily doped P - type layers are also desirable in photocathode applications. A final P layer on a multilayer epitaxial device ensures good ohmic contact as well as lower series resistance.

The need for P-type InP layers for device fabrication, has increased the study of P-type dopants for this material (11). In the present work, magnesium was chosen as the P-type dopant, instead of the more commonly used zinc or cadmium. This is because Mg has high solubility in III-IV compounds, and low diffusivity, which can be important when abrubt junctions or interfaces are desired (12).

Little information exists on the growth and characterization of InP:Mg. Mg not only provides a shallow substitutional monovalent acceptor in InP (13), but also forms complexes with deep level flaws at high doping concentrations as is evident from this work. For efficient performance of the devices, it is essential that the material used be free of defects.

At this juncture, it is worthwhile to mention the types of crystalline defects and their effect on the characteristics and reliability of devices. Crystalline defects can be classified into point defects, line defects and planar defects. The point defects include impurities (foreign atoms) and native defects; dislocations form line defects; and planar defects include grain boundaries and stacking faults. The presence of these defects gives rise to noise or leakage in solid state devices. Defects in the

substrates tend to propagate up into the epilayers during growth. Hence it is important that the material should be as defect-free as possible.

As mentioned earlier, point defects are classified into impurities and native defects. The most common impurities in semiconductors are known commonly as "shallow" impurities or dopants. Dopants are introduced deliberatly into the semiconductor where they form localized donor or acceptor levels. These levels are described by the hydrogenic model and are called "shallow states". These states are characteristically located within 0.1 eV of either band edge.

In InP a number of elements (Cu, V, Fe) have been found to form deep level centers within the gap. They generally have activation energies greater than 0.1 - 0.2 eV and do not follow the hydrogenic model. Other deep states are thought to originate from native defects, or complexes between two or more point defects (14). Shallow impurities are also known to form complexes with other point defects, giving rise to deep levels in the forbidden gap.

A deep defect in a semiconductor may act either as a trap or as a recombination center (15), depending on the

defect, temperature and doping conditions. If a minority carrier trapped at an impurity center lives a mean lifetime in the captured state and is ejected thermally to the band from which it came, the center is regarded as a trap. If, however, before thermal ejection can occur, a majority carrier is trapped, recombination will take place and the defect is a recombination center.

These centers are particularly important in wide band-gap semiconductors because they offer the most likely means of recombination. Hence the lifetime of injected carriers is affected by the presence of deep levels. Traps and recombination centers also tend to limit the diffusion lengths of carriers, and promote non-radiative recombination. Undesired trapping effects change the switching times in devices such as photoconductors and non-radiative recombination process affects the efficiency of light emitting diodes.

To characterize a defect, information about its nature, energy level, capture cross section, density, etc., become essential. As a result several characterization techniques have been developed. The most commonly used methods are photoluminescence (PL) (16), optical absorption (17), Hall effect (18), photo-induced transient spectroscopy (PITS)

(19, 20) and capacitance techniques (1, 21).

The purely optical methods like PL, optical absorption, etc., and Hall effect provide detailed information on shallow levels, but only obscure or no information on deep levels. The strong lattice coupling for deep states and their consequent non-radiative nature complicate optical spectra. So these methods provide little information on deep traps.

The capacitance techniques (1, 21) like thermally stimulated capacitance, photocapacitance, deep level transient spectroscopy; and photo-induced transient spectroscopy (PITS) provide opportunities for the characterization of deep states. These techniques give a quantitative measure of energy level, the capture cross section and the density of deep states. Capacitance methods are much more sensitive than the other methods mentioned above. However, information about the physical and chemical nature of the level is not available directly. Out of the capacitance techniques mentioned, DLTS has an upper hand due to its greater sensitivity, its greater range of observable trap depths and its convenience to use and interpret. PITS, despite several difficulties is found to be suitable for determining deep level traps in highly

resistive semiconductors (22). PITS used to study deep-level flaws in semi-insulating GaAs is given in reference (19, 20).

Deep level characterization of InP done in the past is discussed in chapter II. The theory of DLTS characterization technique used in this study is described in chapter III. The experimental procedures that include CV, IV and DLTS measurements are reported in chapter IV. Finally results and discussions are presented in chapter V.

CHAPTER 2

LITERATURE SURVEY

A survey of literature shows a few experimental measurements of defects in InP. Table I gives a summary of the results obtained from past work. These include defects induced by electron irradiation and by dopants. Irradiation is a convenient way to produce simple defects in a semiconductor mainly to determine the characteristics of the native defects in the material. Previous work (23-30) has shown, using DLTS, that electron irradiation induces several deep centers in InP. The activation energy, capture cross section and the trap density were calculated in each case. Annealing kinetics of these irradiated samples were also studied (24, 27, 28, 30).

Several impurities in III-V semiconductors have been the object of much study in recent years because they often appear as common contaminants or as deliberately introduced dopants in these materials. In either case they tend to behave as deep centers and significantly affect the electronic properties of the host by acting as efficient trapping and recombination centers. Transition metal

TABLE I. A SUMMARY OF RESULTS OBTAINED FROM THE PAST WORK.

Material Type and Growth Methods	Electron Traps		Hole Traps		Proposed Identity of Defects	Method of Measurement	Reference
	Activation Energy (eV)	Capture Cross Section	Activation Energy (eV)	Capture Cross Section			
n-InP Czochralski Method	0.09 0.14 0.22 0.21 0.37 0.7-0.9 0.64	>3.3 >2.7 >2.2 >1.9 >1.7 >1.4 >1.3				DLTS electron irradiation	23
n-InP LPE	0.14 0.16 0.37 0.76	2.0 0.3 150 29,000			Intrinsic Defect Intrinsic Defect Intrinsic Defect Primary Defect	DLTS electron irradiation	24, 30
p-InP LEC			0.37 0.53 0.32	80 50 6	Primary Defect Zn-related Defect Primary Defect	DLTS electron irradiation	24, 30
p-InP LPE			0.17 0.33 0.37 0.53	21 24 17 60	 Primary Defect Primary Defect	DLTS electron irradiation	27
p-InP LEC			0.15 0.34 0.52 0.58	>0.27 >0.19 >0.00033 >0.15	Impur. related def. Primary Defect Primary Defect Primary Defect	DLTS electron irradiation	28
n-InP LPE or LEC	1.13 (Mn) 1.35 (Cu) 0.98 (Cu) 1.20 (Cu)		0.135 (Cu) 0.302 (Cu) 0.690 (Cu)	3.5 22 91	Mn-related defect Cu-related defect	PL PL	32
p-InP			0.21	7	V-related defect	DLTS & DLOS	34, 35, 36
n-InP LEC	0.63 + 0.03					DLTS	37
p-InP LPE			0.22	0.10	Impurity-Phosphor. vacancy complex	DLTS	38

TABLE 1. A SUMMARY OF RESULTS OBTAINED FROM THE PAST WORK. Continued

Material Type and Growth Methods	Electron Traps		Hole Traps		Proposed Identity of Defects	Method of Measurement	Reference
	Activation Energy (eV)	Capture Cross Section $10^{-16}cm^2$	Activation Energy (eV)	Capture Cross Section $10^{-16}cm^2$			
p-InP VPE			0.09 0.22 0.29 0.41 0.50	0.60 0.04 4.00 4.00 3.00	Residual Impurities	DLTS	40
p-InP LEC			0.52		Phosph. Vacancy or Phosph-interstitial related defect	DLTS	41
p-InP LEC			0.15	7.50		Admittance Spectroscopy	43
n-InP LEC, LPE, VPE			0.58 0.78 0.89 1.15		Phosph. Vacancy Phosph. Vacancy Phosph. Vacancy Phosph. Vacancy / impurity complex	Photocapacit. Techniques	44
n-InP LEC	~ 0.80 0.68 0.52 ~ 0.56 0.58 0.40 0.42	600 1500 300 -- 90,000 30 16,000				DLTS	45
n-InP VPE	0.63 0.59 0.43	29 19,000 58				DLTS	46
n-InP LEC	Ec-0.30±0.03 Ec-0.35±0.03 Ec-0.49±0.03 Ec-0.59±0.04	>40 >38 >0.0001 >28			(In-Vacancy, P interstitial) (PIn Antisite or In-Site impurities) (PIn Antisite or In-Site impurities)	DLTS	47

TABLE I. A SUMMARY OF RESULTS OBTAINED FROM THE PAST WORK. Continued

Material Type and Growth Methods	Electron Traps		Hole Traps		Proposed Identity of Defects	Method of Measurement	Reference
	Activation Energy (eV)	Capture Cross Section $10^{-15}cm^2$	Activation Energy (eV)	Capture Cross Section $10^{-15}cm^2$			
n-InP LPE	0.15	>0.09			Metastable defect	DLTS and TSCAP	48, 49
	~ 0.40	--					
	~ 0.40	--					
	0.09, 0.14	>2					
	0.37	>2					
n-InP LEC	0.41	--			Complex of Fe with intrinsic defects or MFe defects	DLTS TSCAP Photocapacit.	52, 56
	0.24	>6					
n-InP	0.12	--			M:P center or a Vp complex	DLTS	53
n-InP LEC	Ec-0.79				Gamma-ray induced defect	DLTS	57
	Ec-0.81						
	Ec-0.41						

impurities like Mn, Cu, Fe, Cr, Ni, Co, etc., (31, 32) form deep levels in InP and are characterized by DLTS.

Titanium, vanadium and iron in InP are of technological importance as these give rise to semi-insulating materials. B. Clerjaud et. al. have performed studies on vanadium doped InP, co-doped with Zn. The traps were characterized by luminescence excitation experiments, DLTS, DLOS (Deep Level Optical Spectroscopy) and absorption experiments (33-36). Deep levels due to titanium were identified for the first time by C. D. Brandt et. al (37) using DLTS. Fe-doped InP also forms deep-centers as shown in reference (38). InP samples intentionally doped with transition metals are found to be contaminated with hydrogen (39). The hydrogen binds with one of the transition-metal-phosphorous ligands. These bonds were observed by infrared spectroscopy. Hydrogen gets incorporated in materials grown under hydrogen atmosphere.

Zinc, the most commonly used acceptor impurity in InP and other related compounds, is found to form deep levels in InP (40, 41). Zn atoms are also seen to interact with native defects shown in (42) using PL and SIMS (Secondary Ion Mass Spectrometry) techniques. Mg, another p-type dopant of InP forms deep traps (43). This trap has been

characterized by admittance spectroscopy. Several deep traps were observed in bulk and epitaxial InP and were characterized by either photocapacitance or transient spectroscopy (44-47).

Another type of defect reported in the literature is the metastable defect in 1MeV electron irradiated InP (48-54). This defect, known as the M-center can exist in either of two configurations, A or B, each with distinct electronic properties. Reversible transformations between configurations can be induced and each configuration is characterized by a distinct deep level transient behavior. The M-center displays both self-trapping and negative-u characteristics due to large lattice relaxation. These properties are discussed in detail in references (50, 51). The MFe center in Fe:InP is characterized by thermally stimulated capacitance, photocapacitance and DLTS (52, 54).

Kennedy and Wilsey have investigated the intrinsic defects in III-V semiconductors using Electron Paramagnetic Resonance (EPR) (55, 56). Using EPR they observed an Indium vacancy (V_{In}) or a complex involving a vacancy and a phosphorous antisite (P_{In}) in both n and p-type material. Although this technique has been very useful in the study of vacancies, interstitials and complexes involving

intrinsic defects in silicon and III-V compounds, its use has been limited due to difficulties in interpretation of data.

Besides electron iraradiation, Gamma-ray irradiation is also used to induce defects in semiconductors. Defects introduced by 1MeV gamma-rays in InP were characterized using DLTS (57). Annealing experiments were also performed on these samples.

CHAPTER - 3

THEORY OF DLTS

Deep level transient spectroscopy (DLTS) (1) originally developed by D. V. Lang is a powerful tool to study defect-induced trap states in the bandgap of semiconductors which are at least 0.1 eV from either band edge. This method uses the capacitance of a Schottky barrier or a p-n junction as a probe to monitor the changes in the charge state of a center as a consequence of the capture and emission of carriers that take place.

A summary of the capture (c) and emission (e) processes which characterize a deep trap in p-type material is shown in Fig (2). e_1c_1 and e_2c_2 refer to the rates for minority (electrons) and majority (holes) carriers respectively. In the quiescent state of the system, the diode is reverse biased and the observable traps are in the depletion region. As this region is devoid of mobile carriers, the capture rates are zero and the equilibrium steady state electron occupation (n) of the level is determined by the thermal emission rates e_1 and e_2.

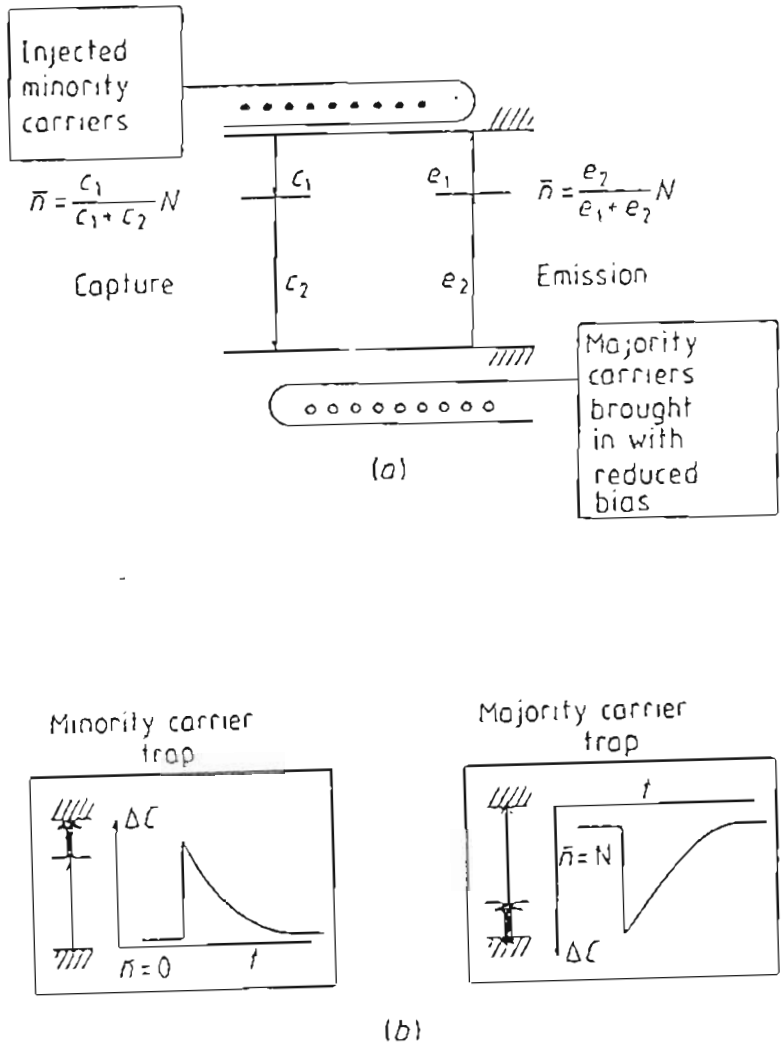

FIG 2. Capture and emission processes.

Hence,

$$n = [e_2/(e_1+e_2)]\ N \quad \text{----------(1)}$$

where N is the trap concentration. This value of n can be changed by applying a bias pulse to introduce carriers, which in turn alters the capacitance C. A schematic of this test sequence is shown in Fig.(3). At time $t = t_{p1}$ the bias pulse of width $(t_{p2} - t_{p1})$ is introduced. The steady state electron occupation during the bias pulse is given by;

$$n = [C_1 / (C_1 + C_2)]\ N \quad \text{----(2)}$$

After the pulse is removed and the diode is returned to its quiescent state (after t_{p2} in Fig.(3)), this population slowly returns to equilibrium as a result of the thermal emission of the trapped carriers. As the trapped carriers are emitted, the quiescent value of the capacitance is re-established. One of the emission rates e_1 or e_2 usually dominates, depending upon the proximity of the trap to a band edge. Furthermore, if a Schottky diode is used, $e_2 >> e_1$ as injection of minority carriers is impossible unless stimulated by a photon. The thermal emission rate of trapped carriers can be expressed by,

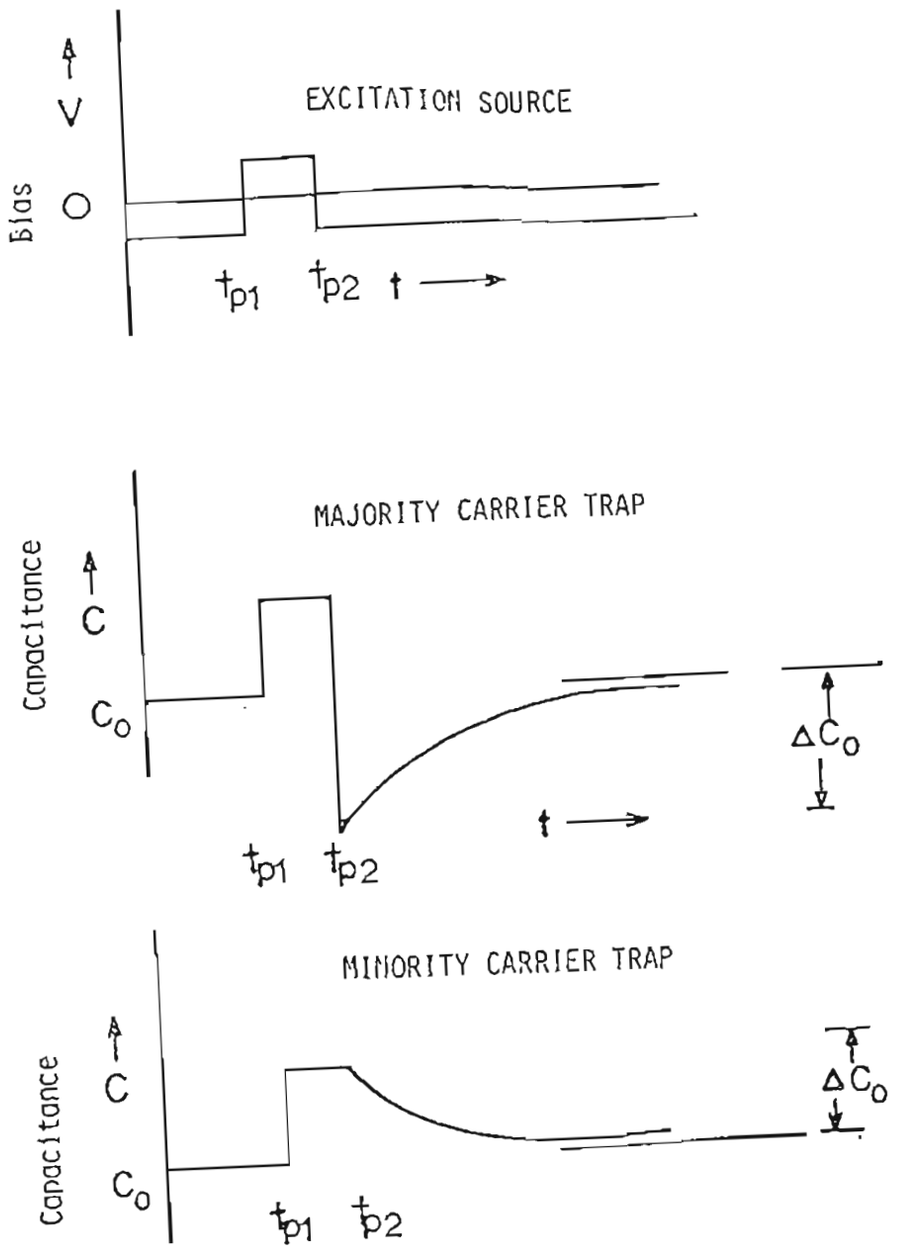

FIG. 3. A schematic of DLTS pulse sequence.

$$e_p = N_v V_p \sigma_p \exp(-E_A/KT) \text{ for holes } ---(3)$$

where,

e_p is the hole emission rate (e_2, in Fig. 2)

N_v is the effective density of states for valence band

$N_v = 2(m_v KT/2\pi h^2)^{3/2}$

V_p is the thermal velocity

$V_p = \sqrt{[3KT/m^*_h]}$

σ_p is the temperature independent capture cross section

E_A is the activation energy

A similar expression holds for the emission of electrons.

The most important feature of DLTS is the ability to display the time constant of the decaying signal by setting a "rate window". This is done by tuning the measurement system to respond only to a transient of a particular time constant. Thus, if the emission rate of a trap is varied by varying the sample temperature, the instrument will show a response peak at the temperature where the trap emission rate equals that of the tuned rate window. Fig.(4) illustrates the rate window concept.

The rate window may be produced by a number of methods

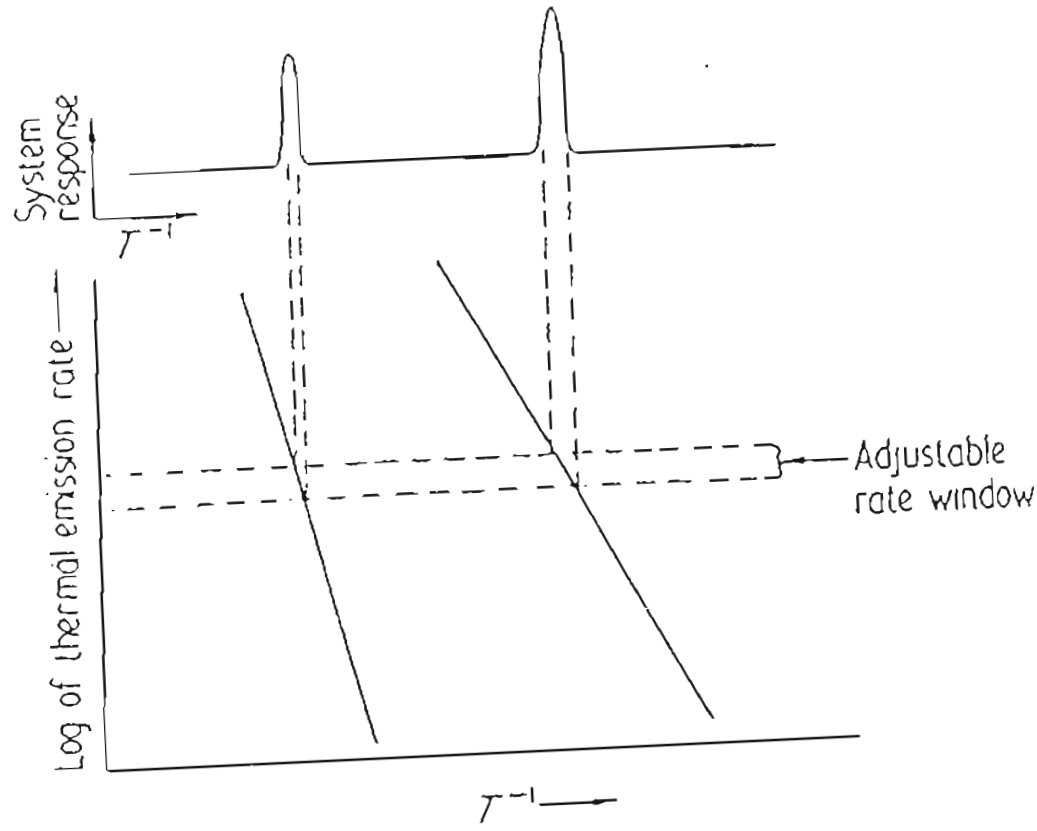

FIG. 4. The DLTS rate window concept

such as a lock-in-amplifier, a band-pass filter, a double box car integrator, etc., The method originally proposed by D. V. Lang made use of the dual gated integrator (double box car). This device measures the transient signal at preassigned instants t_1 and t_2 after the bias pulse and records the analog difference $[C(t_2)-C(t_1) = \Delta C]$ as a function of temperature to produce a DLTS spectrum. This is illustrated graphically in Fig.(5). The resulting signal ΔC, can be expressed as

$$\Delta C = \Delta C(0)\ S(e^*) \text{ ------ } (4)$$

where $\Delta C(0)$ is the capacitance change due to the pulse at $t = 0$. And, for exponential transients,

$$S(e^*) = \exp(-e^* t_1) - \exp(-e^* t_2) \text{ --- } (5)$$

Differentiating equation (4) with respect to e^* and setting the result equal to zero, the thermal emission rate corresponding to the peak of the DLTS signal can be obtained and the resulting equation is

$$e^* \approx \ln(t_2/t_1)/(t_2-t_1) \text{ -------- } (6)$$

Making several scans at various values of t_1 and t_2,

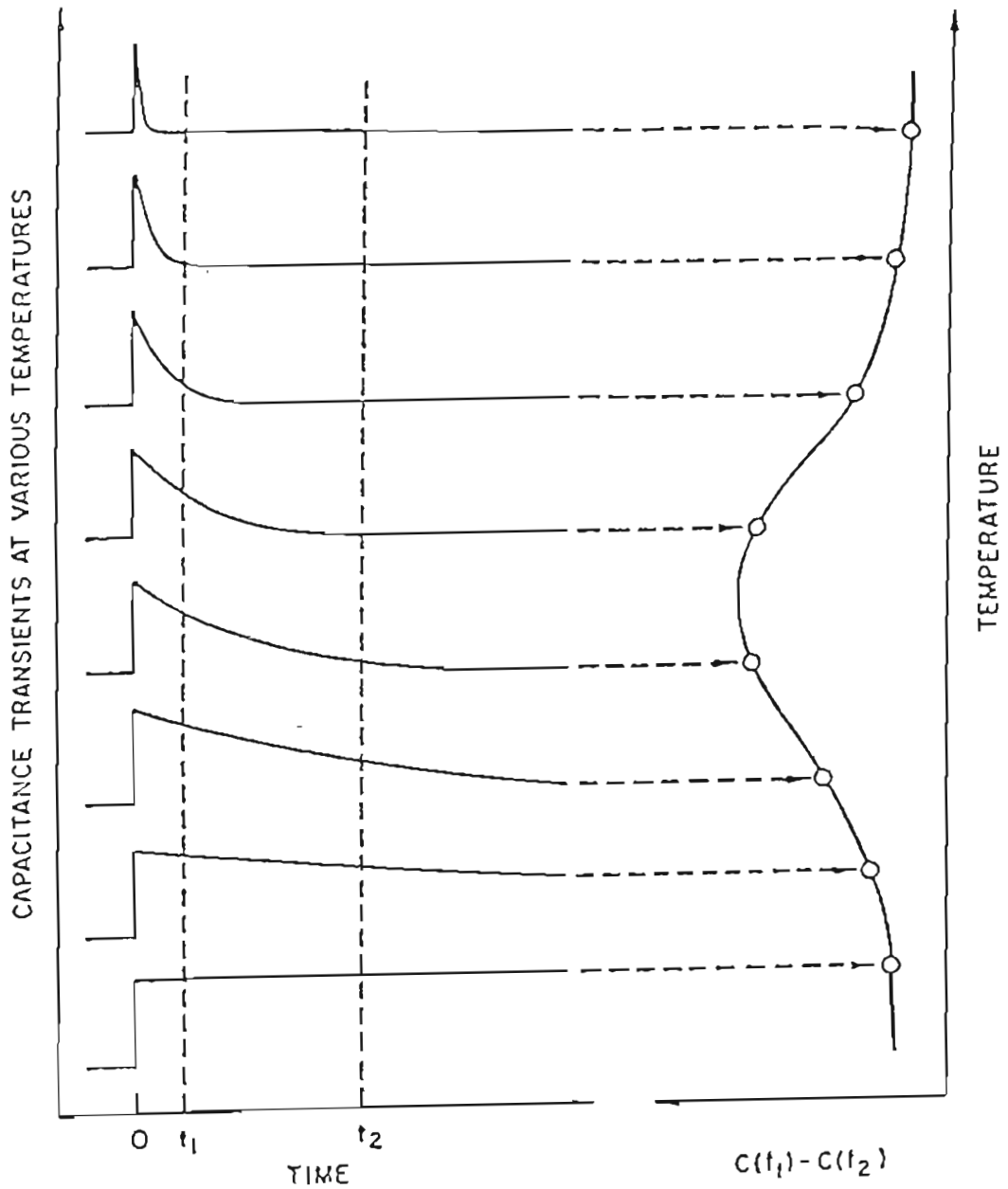

FIG. 5. Illustration of how a double boxcar is used to define the rate window. The left-hand side shows capacitance transients at various temperatures, while the right-hand side shows the corresponding DLTS signal resulting from using the double boxcar to display the difference between the capacitance at time t_1 and the capacitance at time t_2 as a function of temperature.

while keeping the ratio t_2/t_1 constant, one obtains corresponding values of T^*, the temperature at which $e_p = e^*$ for the trap. In other words, changing the rate window (e^*) to lower (higher) rates shifts the spectrum to lower (higher) temperatures. Plotting the values e^* and T^* in an Arrhenius form as shown in Fig.(4), the activation energy and capture cross section in equation (3) can be measured from the slope and intercept of the plot.

The trap concentration can be obtained using the expression (1, 67)

$$N_T = 2[\Delta C(0)/C]\,[N_A-N_D] \quad \text{---------- (7)}$$

for $N_A-N_D \gg N_T$

$$= [(\Delta C(0)/C+1)^2-1]\,[N_A-N_D] \quad \text{------- (8)}$$

for $N_A-N_D \sim N_T$

where N_T is the trap concentration, C is the capacitance of the diode under quiescent reverse-biased conditions. N_A-N_D is the net acceptor concentration in the p-type material and is determined by using CV analysis. The values of C and N_A-N_D are known and $\Delta C(0)$ can be calculated using equations (4) and (5).

CHAPTER - 4

EXPERIMENTAL PROCEDURE

The p-type InP samples used for the DLTS investigation were grown in Oregon Graduate Center using OMVPE. The layers were grown on semi-insulating substrate using trimethyl indium (TMIn) and phosphine (PH_3) at atmospheric pressure. The magnesium dopant used was bis-cyclopentadienyl magnesium (Cp_2Mg). Relative mole fractions are given in Table II. Resulting layers were 3-4 microns thick. The details of growth are in reference (58). The DLTS characterization is discussed in reference (59).

Ohmic contacts to p-type InP were formed by evaporation of a 90/10 Au/Zn alloy through masks, followed by a two minute anneal in argon at 450°C at atmospheric pressure. Indium dots were rubbed onto the contacts and then annealed at 150°C for one minute. For evaporation 35 mg of the alloy was used. The source was 4 cm from the sample and a shutter blocked the sample until evaporation began. The samples were covered by masks with four holes, 0.75 - 1 mm diameter, in a square pattern. The sample was allowed to cool prior to exposure to air. All contacts were

TABLE II. Growth Parameters for OMVPE InP : Mg
(Growth Temperature 600°C)

Sample Number	Mole Fractions		$[PH_3]/[TMIn]$	H_2 l/min
	TMIn	CP_2Mg		
InP 20	4.1×10^{-5}	3.2×10^{-8}	80	8
InP 23	8.3×10^{-5}	4.6×10^{-8}	80	8
InP 57	5.5×10^{-5}	6.5×10^{-8}	105	4
InP 59	5.5×10^{-5}	1.6×10^{-8}	105	4
InP 61	5.5×10^{-5}	4.8×10^{-8}	105	4

verified to have a linear current/voltage relationship continuously through positive and negative current values, using a Tektronix 576 curve tracer. Fig. (6) shows the typical I/V relationship for an ohmic contact.

For CV and DLTS analysis, Schottky barriers were prepared on InP by evaporating gold through a mask in high vacuum (10^{-4} Torr). Again the masks used had holes of 0.75 - 1 mm diameter. The current /voltage characteristics of the Schottky diode is observed using a Tektronix 576 curve tracer. Fig.(7) shows the IV curve of a typical metal-semiconductor contact and Fig.(8) the energy band diagram.

The room temperature capacitance versus voltage (CV) data are taken using a 1 MHz test frequency. The sample was mounted on a micromanipulator. The relationship between C and V is given by (60),

$$C = \sqrt{[\{e\epsilon_s(N_A-N_D)A^2\}/\{2(V_{bi}-V)\}]} \quad F/cm^2 \quad --(9)$$

where N_A-N_D is the net acceptor concentration,

V_{bi} is the built-in potential.

V is the applied voltage

e is the electronic charge

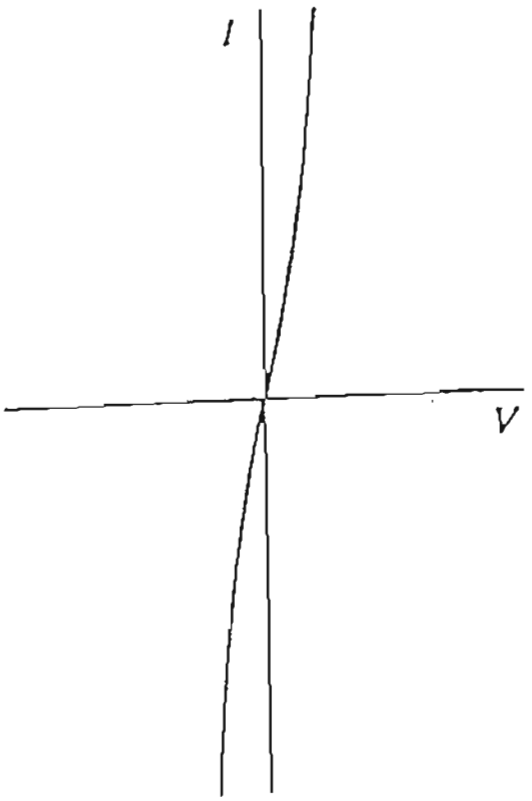

FIG. 6. IV curve of ohmic contact.

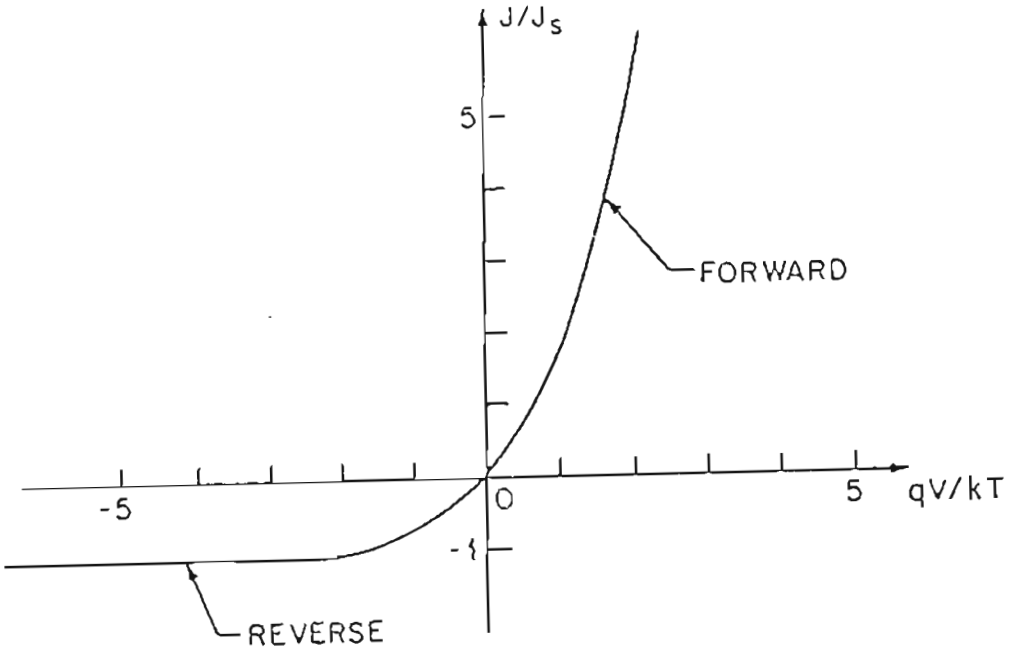

FIG. 7. IV curve of Schottky contact.

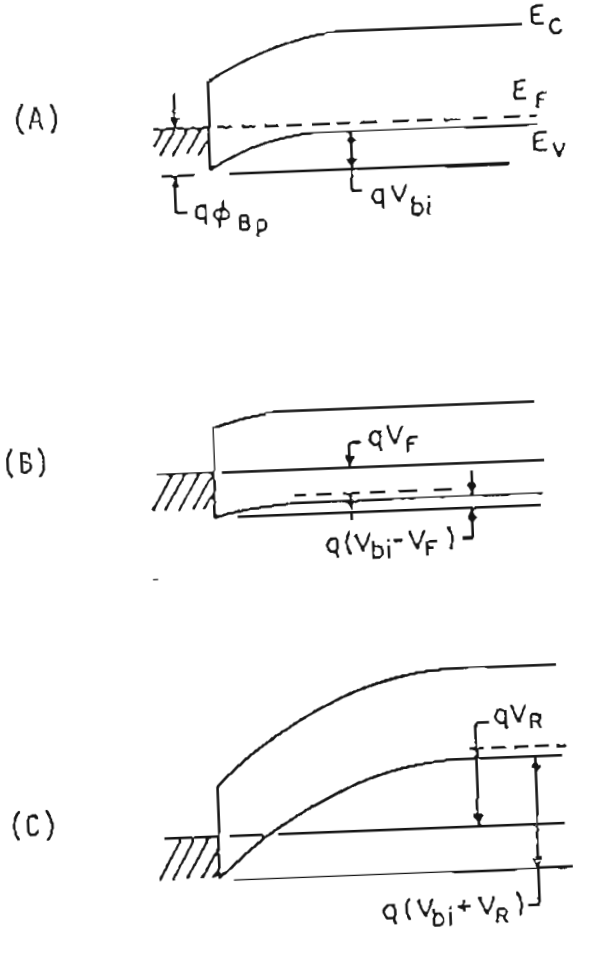

FIG. 8. Energy - Band diagram of metal p-type semiconductors under different biasing conditions (A) Thermal equilibrium. (B) Forward bias. (C) reverse bias.

$\epsilon_s = \kappa \epsilon_0$

κ is the dielectric constant of the semiconductor

ϵ_0 is the permittivity of free space.

A is the area of the diode.

Equation (9) can be re-written as,

$$1/C^2 = 2(V_{bi}-V)/e\kappa\epsilon_0(N_A-N_D)A^2 \text{ ------- (10)}$$

Plotting $1/C^2$ versus V yields a straight line if N_A-N_D is constant throughout the depletion region. From the slope of the line the carrier density can be calculated as follows,

$$-d(1/C^2)/dV = 2/[e\kappa\epsilon_0(N_A-N_D)A^2]$$

or

$$N_A-N_D = [2/(e\kappa\epsilon_0A^2)]\ [-1/\{d(1/C^2)/dV\}] \text{ --------(11)}$$

The intercept on the voltage axis corresponds to the built in voltage (V_{bi}) and hence the barrier height (ϕ_b) can be determined using the relation

$$V_{bi} = \phi_b - V_p \text{ ---------------(12)}$$

where V_p is the potential difference between the Fermi level (E_F) and the valence band (E_V), which can be deduced from the impurity concentration as follows,

$$V_p = (KT/e) \ln (N_v/N_A) \text{ ---------- (13)}$$

where,

N_v is the density of states for valance band

K is the Boltzmann constant

N_A is the impurity concentration

In addition to the CV analysis, current voltage (IV) behavior of the Schottky diodes were studied on the basis of thermionic emission theory. The basic Schottky model for IV relationship is given by the equation,

$$J = J_s [\exp (eV/nKT) - 1] \text{ ---------- (14)}$$

here,

J is the current density

J_s is the reverse saturation current density

n is the ideality factor

V is the applied voltage

e is the electronic charge

K is the Boltzmann constant

T is the temperature

J_s is determined from the thermionic emission over the barrier ϕ_b and can be written as,

$$J_s = A^* T^2 \exp(e \phi_b/KT) \text{ ---------- } (15)$$

and A^*, the effective Richardson constant is given by,

$$A^* = (4 \pi e m^* K^2) / h^3$$

m^* being the effective mass and h Plank's constant. Taking logarithm of equation (14) we get,

$$\ln J = \ln J_s + eV/nKT$$

Plotting ln J versus V, gives a straight line with e/nKT as the slope and ln J_s as the intercept. From these two values the ideality factor n and the barrier height ϕ_b can be calculated.

Deep level transient spectroscopy measurements on InP samples were made on Schottky diodes. The diodes were mounted on TO-18 headers and placed in a liquid nitrogen cooled crystal (Oxford Instruments), which has the

capability of scanning temperature from 77°K to 500°K. The measurement system is shown in Fig.(9). A modified Boonton 72BD capacitance bridge was used with a 1 MHz test frequency. The output signal of the bridge was digitized using a storage scope (Tektronix 7D20) with averaging capabilities. The averaged signal was then sent to a computer (Tektronix 4050) for storage and analysis.

The data consist of records of a series of capacitance transients at various temperatures. The stored transients are sampled at different times, providing different rate windows using the two channel boxcar method. The ratio of the two sampling times t_1 and t_2 was maintained constant, such that t_2/t_1 was equal to 4. The data are fitted with the corresponding peak maxima to the equation for hole emission rate using the least square method. A semilog plot of the thermal emission rate versus 1000/T gives the Arrhenius plot of the trap levels. The thermal activation energy is calculated from the slope and the capture cross section from the intercept of the resulting straight line.

Figure (10) represents the Arrhenius plot of FET6AF which is Si^+ implanted GaAs sample and is used as a calibration standard in this work. EL2 denotes the electron

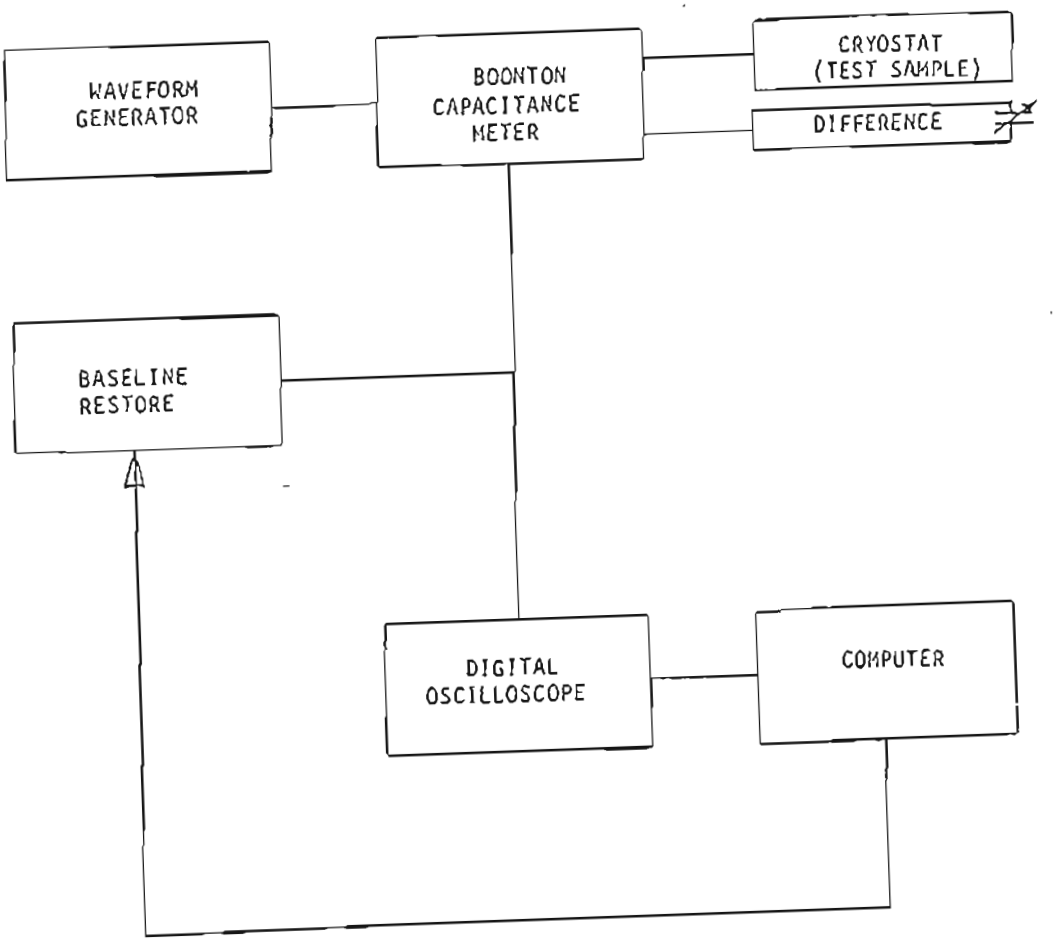

FIG. 9. Block diagram of the measurement system.

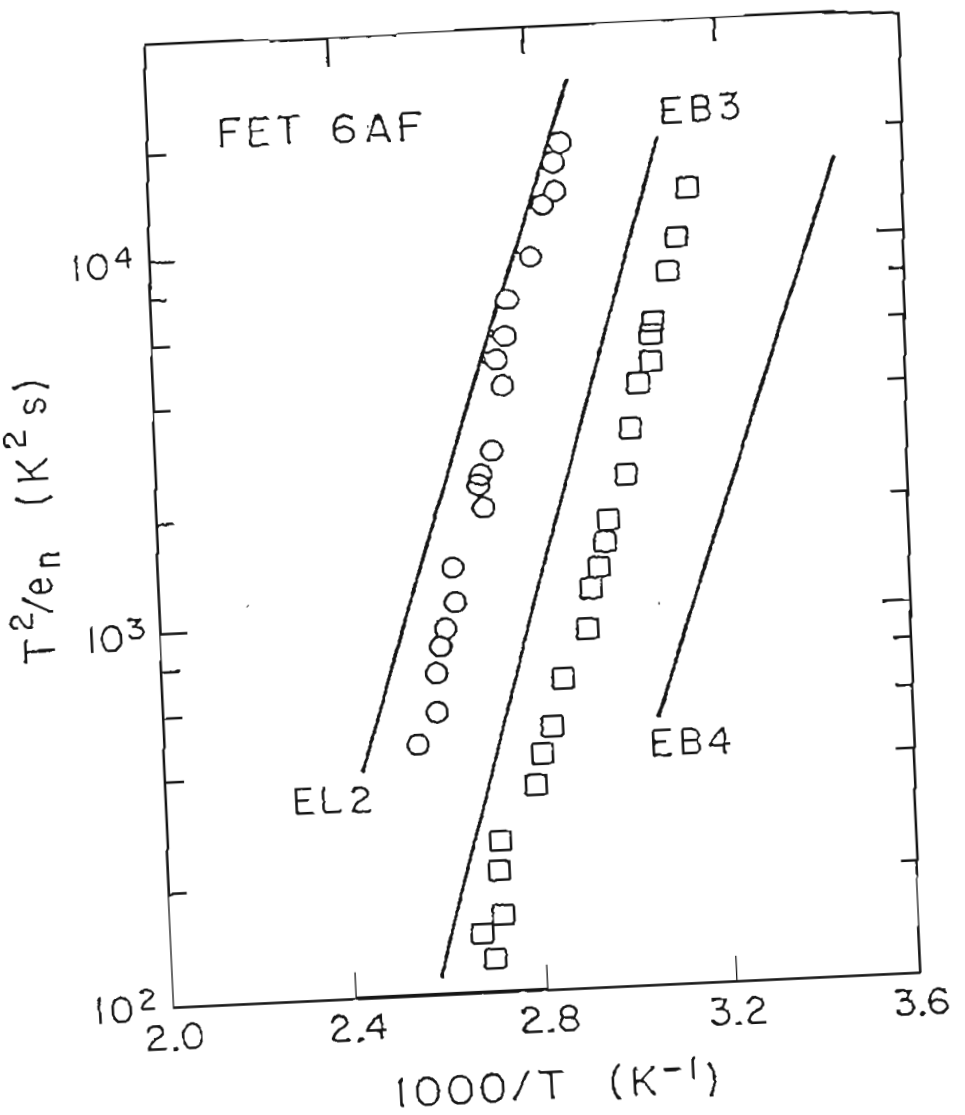

FIG. 10. Calibration Standard.

trap in VPE grown GaAs, measured by Martin et. al. (61). EB3 and EB4 are defects from ion-implantation reported by Bell labs (61). Open circles and squares are data points taken by using the OGC DLTS system. The points do not fit the calibration line because of field enhanced emission. When the doping level exceeds 10^{17} cm^{-3} and the applied voltage is above -3V, the electric field has a great influence on the thermal emission rate of trap. Reference (62) has a detailed discussion of electric field effects on thermal emission of traps in semiconductor junctions. As a result highly doped material could not be characterized by the DLTS measurements. Low doped material exhibited Metal Insulator Semiconductor (MIS) behavior. Hence there were problems in measuring both low and high doped materials by DLTS.

CHAPTER 5

RESULTS AND DISCUSSIONS

As discussed in the previous chapter, CV and IV measurements were used to study the electronic properties of InP epitaxial layers.

CV Analysis

The CV measurements were employed to determine the carrier concentration using equation (10). Fig. (11A and B) show the results of $1/C^2$ versus V for samples InP-23, InP-20 and InP-59. The deviation of these curves from straight lines might be due to stray capacitance, leakage current or high series resistance . The problem of series resistance is more serious in thin epitaxial layers on insulating substrates. Deep levels also commonly distort the profile due to trapping effects. The net carrier concentration was calculated using the linear portion of $1/C^2$ Versus V plot and these values are tabulated in Table III. Acceptor concentrations for the Au-InP diodes range from 10^{15}-$10^{12}cm^{-3}$, and tend to be quite low for several of the diodes.

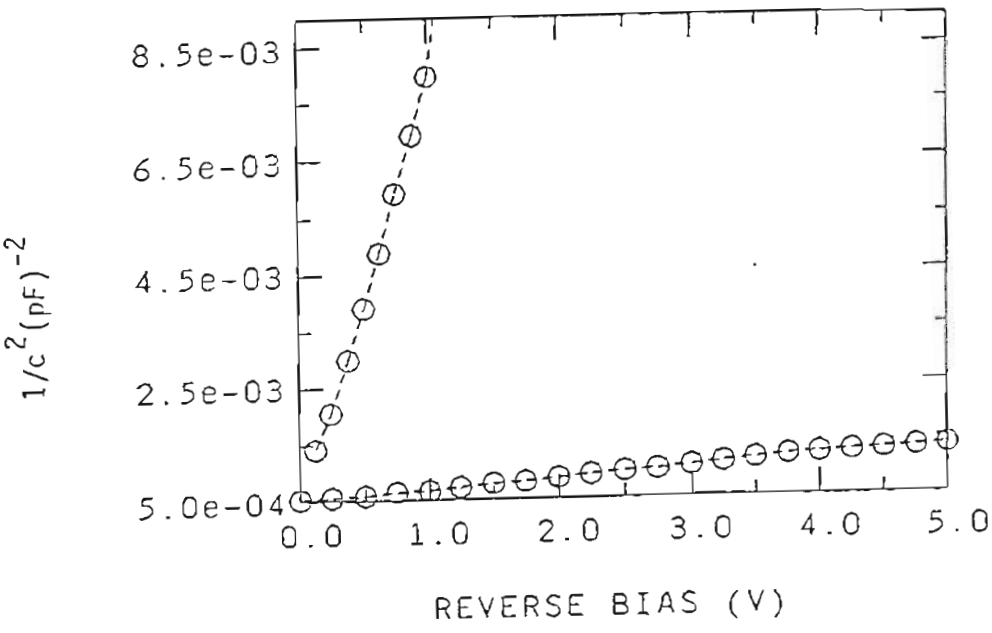

(A)

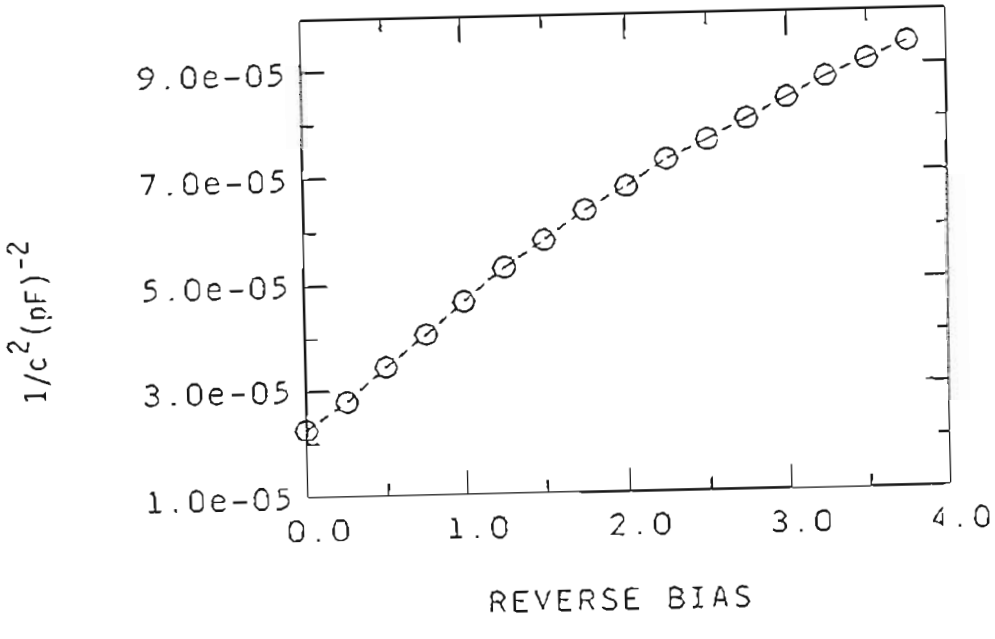

(B)

FIG. 11. $1/C^2$ Versus Voltage

The intercept of $1/C^2$ Vs. V with the abcissa yields values for the built-in voltage (V_{bi}). This voltage is represented schematically in Fig. (8). It is related to the barrier height ϕ_b, by the relation given in equation (12), namely,

$$\phi_b = V_{bi} + V_p$$

where V_p is the distance of the Fermi level from the valence band and can be calculated using equation (13). In equation 12, the Schottky barrier lowering term has been neglected. The barrier height ϕ_b has been calculated for well-behaved Schottky diodes and is shown in Table III. This is done because the values of ϕ_b are reliable for the diodes that do not exhibit MIS behavior. For instance, the barrier height of InP-23 is calculated to be 0.75 eV which is in agreement with the 0.76 eV measurement made on vacuum cleaved material reported in reference (60).

The CV curve of the lighter-doped material exhibited MIS-like behavior. Fig. (12) represents the typical high frquency response of a MIS structure. The doped semiconductor is most probably the area directly under the annealed ohmic-contact and the insulator is that under the

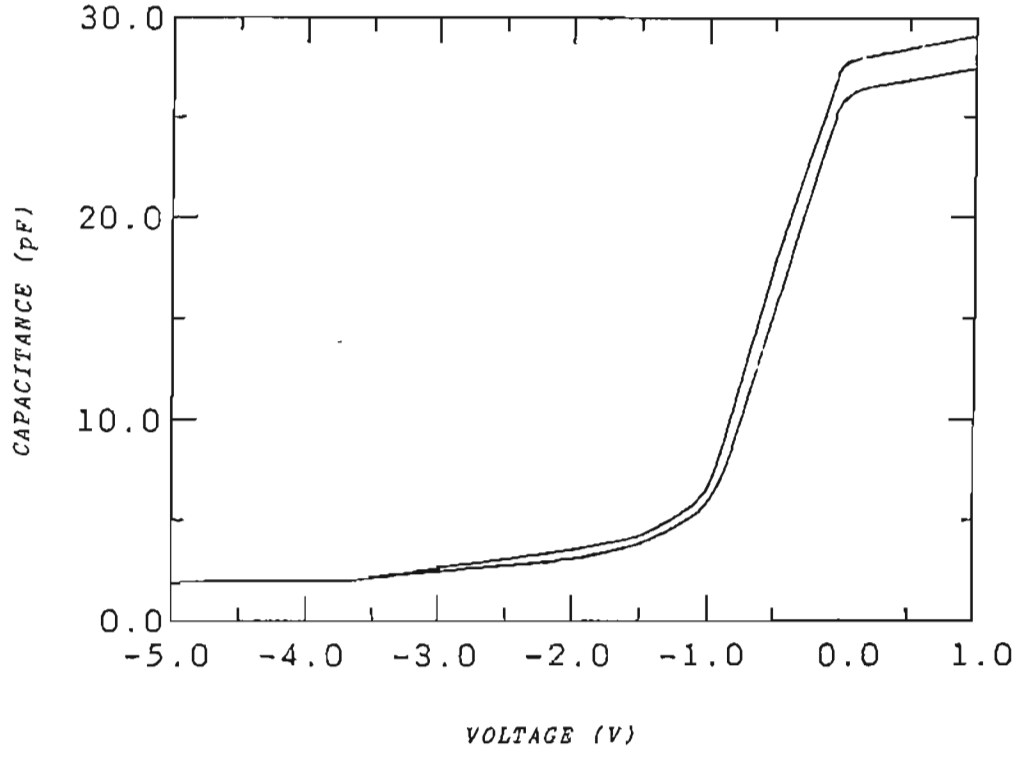

FIG. 12. Capacitance Vs. Voltage exhibiting Hysteresis effect.

TABLE III. Carrier concentration and barrier height calculations from CV analysis.

Sample Number	N_A (Cm^{-3})	V_{bi} (eV)	ϕ_b (eV)
InP 20	4.19×10^{15}		
InP 23	7.32×10^{15}	0.50	0.75
InP 57	5.62×10^{13}		
InP 59	2.09×10^{12}		
InP 61	5.97×10^{14}		

Schottky contact. Due to the capacitance associated with the insulator, a plot of $1/C^2$ Vs. V cannot be used to obtain meaningful values of barrier height (63). However, the functional form of equation (10) holds as long as the diode is operated in the depletion mode and the slope of $1/C^2$ Vs. V plot is still the same as that given in equation (10). This analysis gives a value of N_A of $2x10^{12}cm^{-3}$ for InP 59, as indicated in Table III.

Figure (12) also exhibits hysteresis. This effect was observed in all the diodes and is most likely due to deep levels in theinsulator or is due to defects existing at the interface between InP semi-insulating substrate and InP epitaxial layers.

Unlike the other diodes in Table III, the $1/C^2$ Vs. V curve of InP-61 was not a straight line indicating a non-uniform doping profile. This is probably due to the effect of the depletion region meeting the semi-insulating (SI) substrate which in turn increases the series resistance that is inherent in the case of epitaxial layers grown on SI substrates. As the InP samples are p-type epilayers grown on SI substrates, there exists a depletion region between the substrate and the epilayer. Although, these InP epilayers are 3-4μm thick, for low-doped

material the depletion region extends all the way to the substrate with increasing reverse bias. This causes anomalies in CV profiling because the measured capacitance is less than the actual depletion layer capacitance. The CV analysis in the presence of series resistance is given in reference (64). However in this work, for Inp 61, a tangent was drawn on the $1/C^2$ Vs. V plot to calculate the values of N_A. The value is included in Table III.

Next, a log-log plot of the net acceptor concentrations obtained using CV, as a function of CP_2Mg input flux is shown in Fig. (13). This does not agree with the results reported in the photoluminescence (PL) study, done by F. R. Bacher (58, 59), on some of the samples used in this work. In the latter method, the net carrier concentration was derived from the PL linewidth measurements, which is shown in Fig.(14).

Acceptor concentrations from photoluminescence linewidths are determined from calibrated standards. These standards are samples in which the acceptor concentration has been determined using other techniques, like Hall Effect. Hall Effect is a measurement of the hole carrier concentration and not that of net acceptor concentration and hence is temperature dependent. The PL linewidths, on the other hand depend upon the Donor-Acceptor and

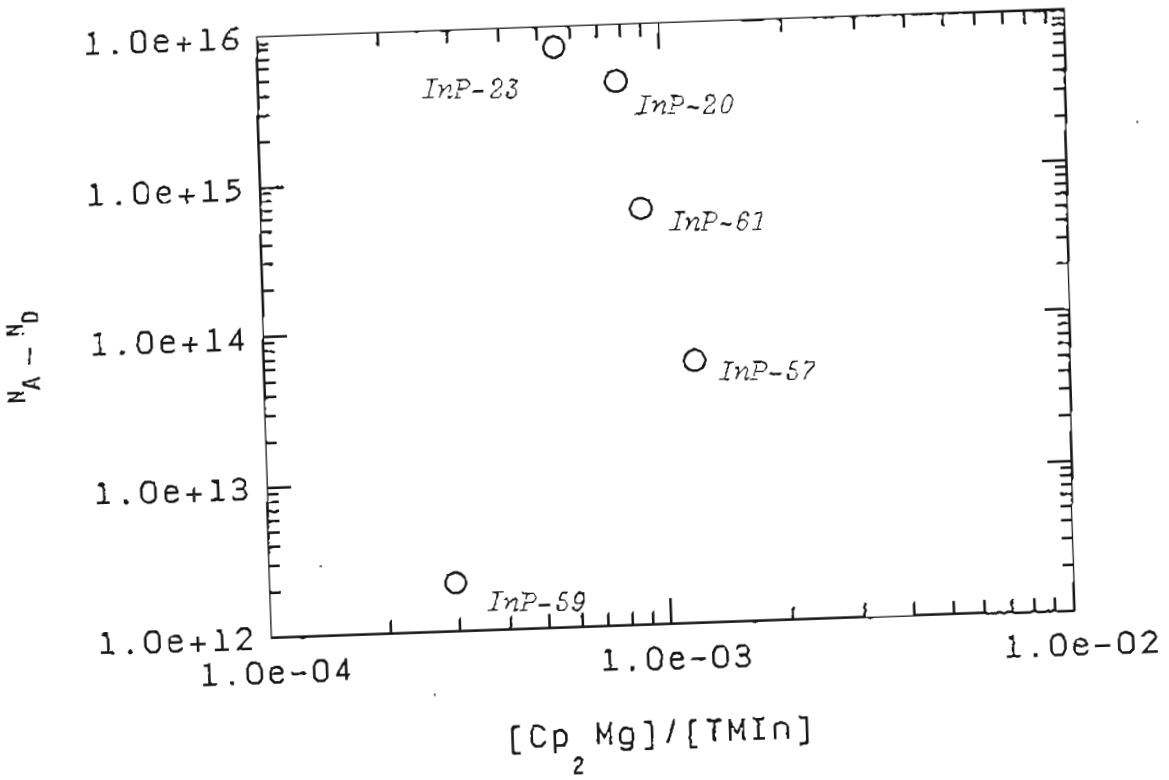

FIG. 13. Net acceptor concentration in InP:Mg Vs. Cp_2Mg/TMIn ratio using CV analysis.

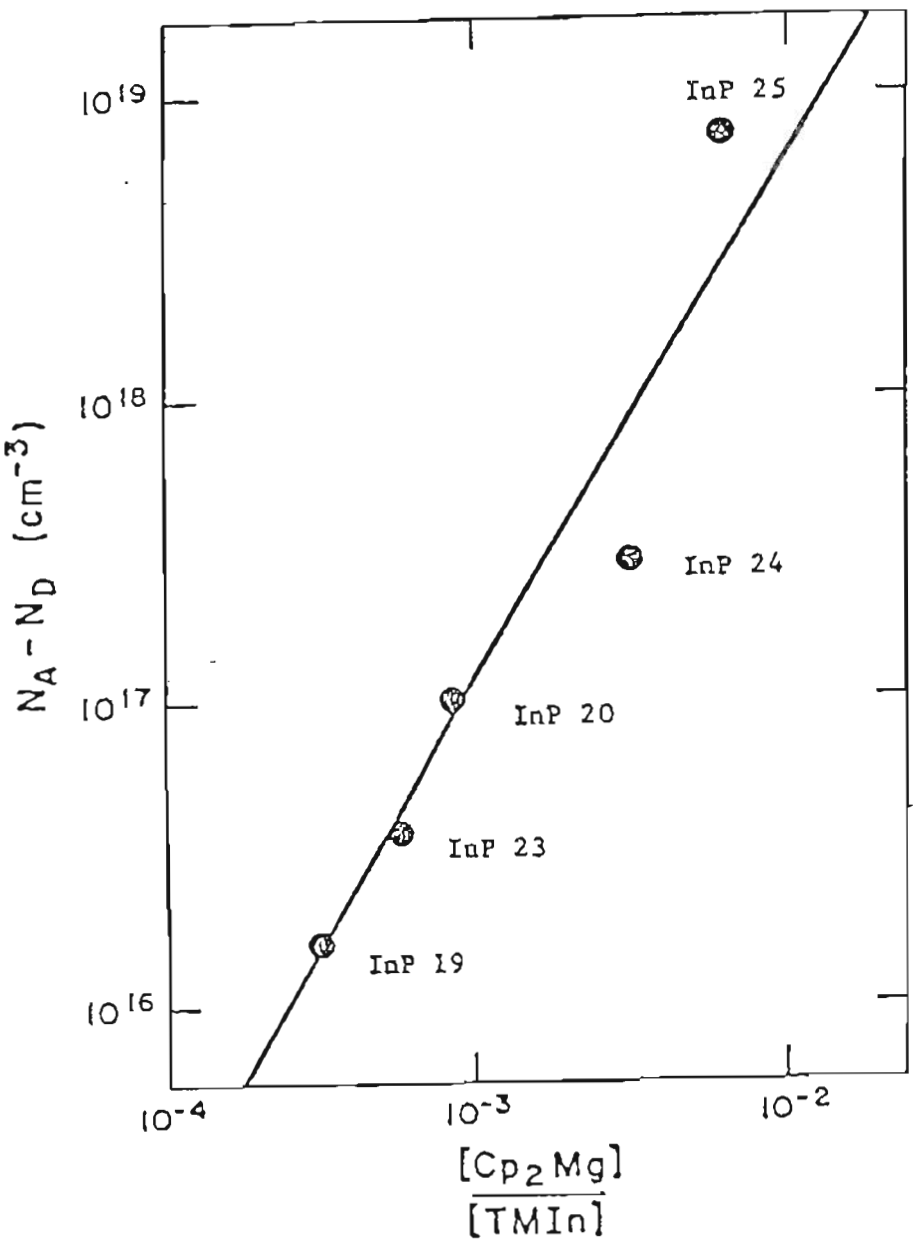

FIG. 14. Net acceptor concentration in InP:Mg Vs. Cp_2Mg/T_{Min} ratio .

Conduction band-Acceptor transitions which are transitions that cannot be separated and, are dependent on the values of both N_A and N_D. These transitions are related to acceptor banding and the movement of the Fermi level into the band. This happens when the material is doped heavily to degeneracy ($>10^{18}cm^{-3}$) and hence this technique is not accurate for concentrations below $10^{16}cm^{-3}$.

CV measurements are also weak, in that the actual area cannot be determined accurately. Equation (10) depends on the square of the area and on N_A-N_D as well. Because the area of Au-InP diodes used is quite large (1 mm diameter), small inhomogeneities of the acceptor concentration may exist under the diode. Inhomogeneities in the Au layer thickness may also exist. The large areas of less charge (small N_A) have a dominant effect on the capacitance and smaller areas of greater charge have minimal effect. The exact extent of this effect is difficult to model. This is because the magnitude of the inhomogeneities in the acceptor concentration of the sample causing fluctuations in the charge under the diode is not clear. Even with these problems involved in the CV measurements the net acceptor concentration calculated by this method can be taken to represent an average of N_A in the diode.

IV Analysis

The IV data was used to calculate the barrier height (ϕ_b) and the ideality factor (n) using equations (14, 15). Fig. (15) shows the IV characteristics of one of the samples. ϕ_b and n were calculated to be 0.49V and 3.1 respectively. The large deviation of the ideality factor from unity is probably due to ohmic losses from Au-Zn ohmic contact. Low resistance contacts to p-type InP are not easily obtainable (65).

Comparing the values of ϕ_b calculated from both IV and CV measurements, it is seen that ϕ_b is considerably less in the former method. This discrepancy may again be due to inaccuracy in the measurements of the effective area of the diode. In CV analysis, as was mentioned earlier, a small area of high charge under the diode has only a small contribution to the total capacitance. In the case of IV analysis, however, the effect is opposite. The area of the diode which has a larger density of accepters has a lower resistance, which may act as a direct shunt for current flow. This effect also depends on the area of the inhomogeneity. Thus the measured area in the IV analysis is not the true area of the diode. Reference (66) shows this type of discrepancy

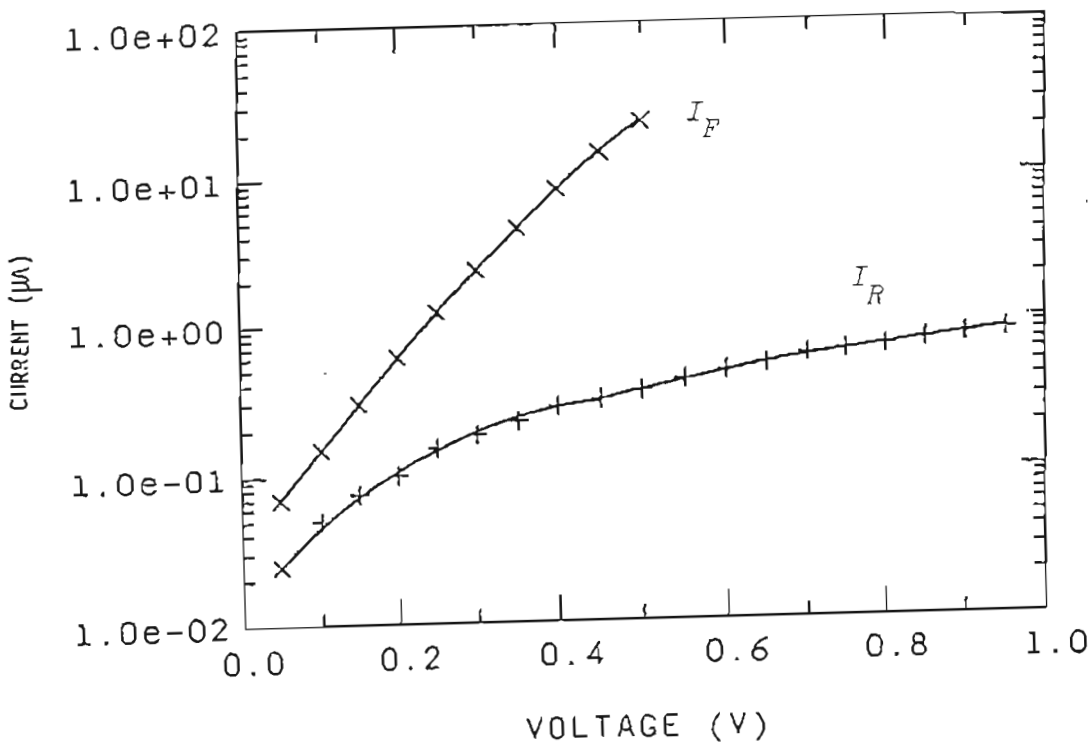

FIG. 15. IV Characteristics.

where the value of ϕ_b measured by CV is greater than that measured by IV.

Defects in InP:Mg

A photoluminescence study was done by F. R. Bacher on some of the InP:Mg samples which revealed the presence of deep levels at doping concentrations higher than $10^{17}cm^{-3}$ (58, 59). Fig. (16) represents the PL spectrum of OMVPE InP:Mg. The measurement temperature for each sample was 77^0K. The broad emission seen in spectra (e) corresponds to Mg-related deep defects in the bandgap. These transitions peaked further interest in the deep defect structure of InP:Mg. However photoluminescence does not give any information on the concentration of these levels or trap parameters such as capture and emission information and therefore DLTS measurements were performed.

Figure (17 A-C) show the DLTS spectra of medium-low doped InP:Mg samples. These represent the spectra of different samples doped with various amounts of Mg. The rate window used for the measurement of the spectra in Fig. (17 A-C) is $5.863x10^{-2}s^{-1}$.

Three different peaks are observed around the same

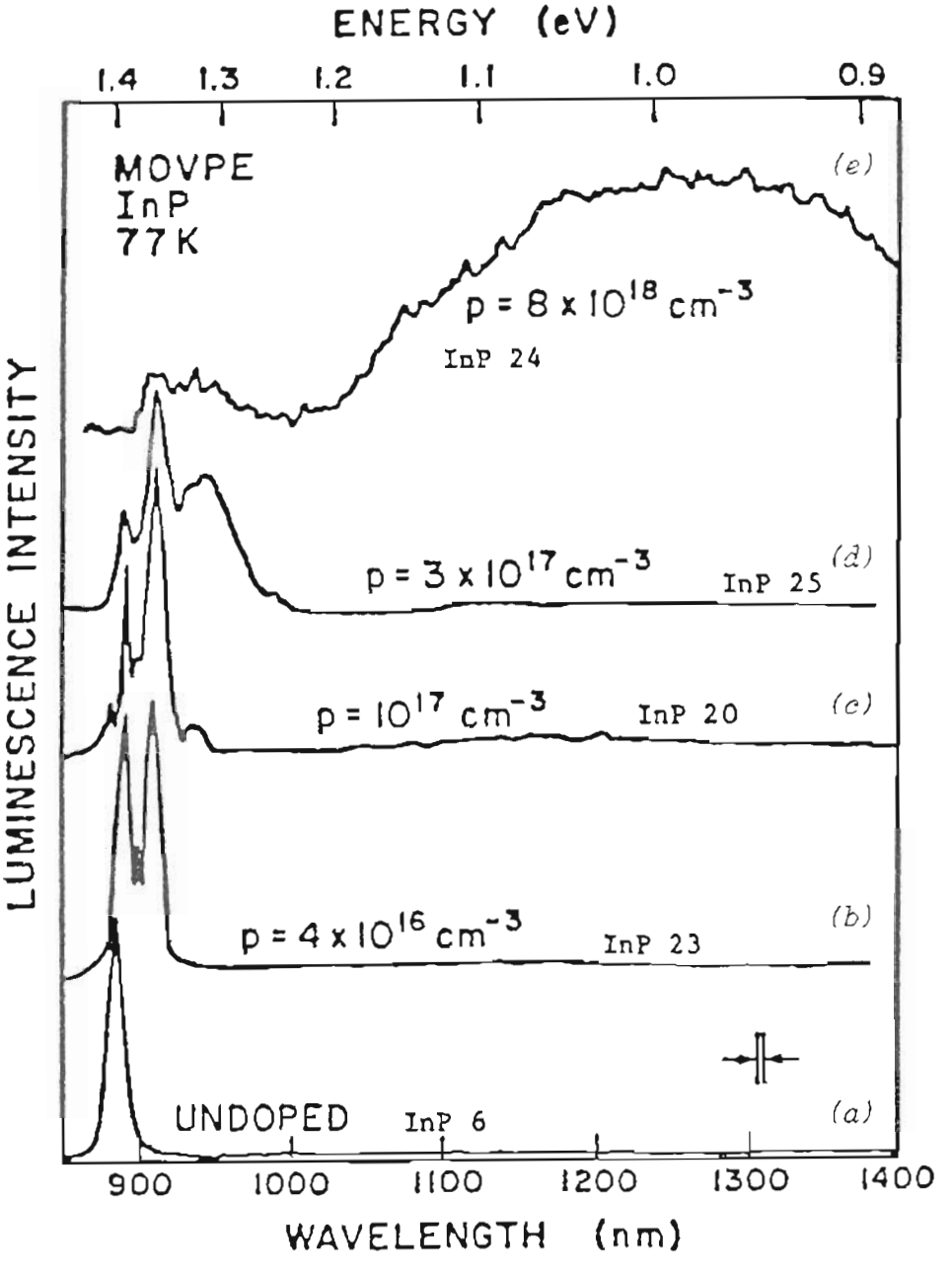

FIG. 16. Photoluminescence Spectrum of MOVPE InP:Mg.

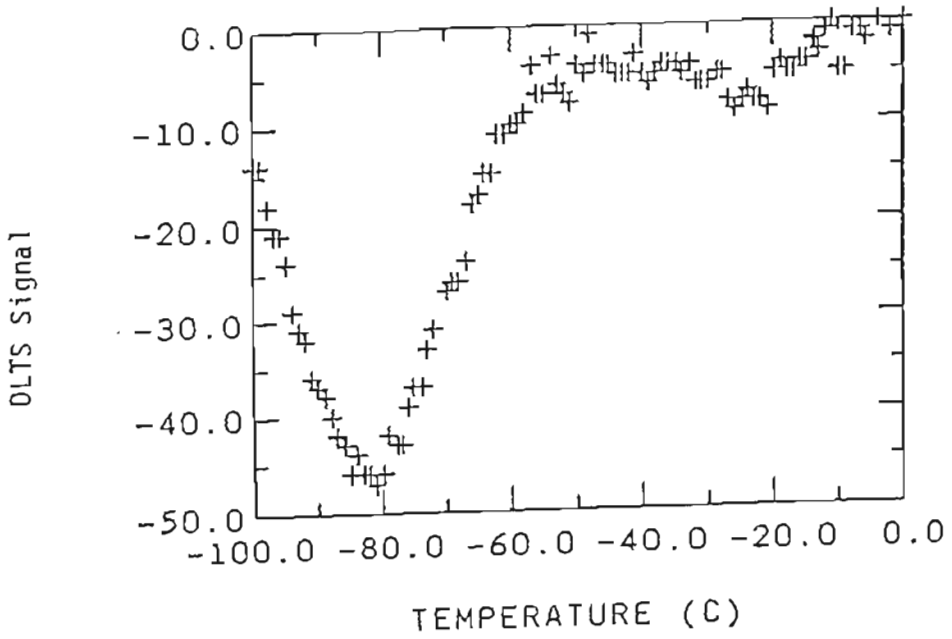

FIG. 17A. DLTS plot of InP-20.

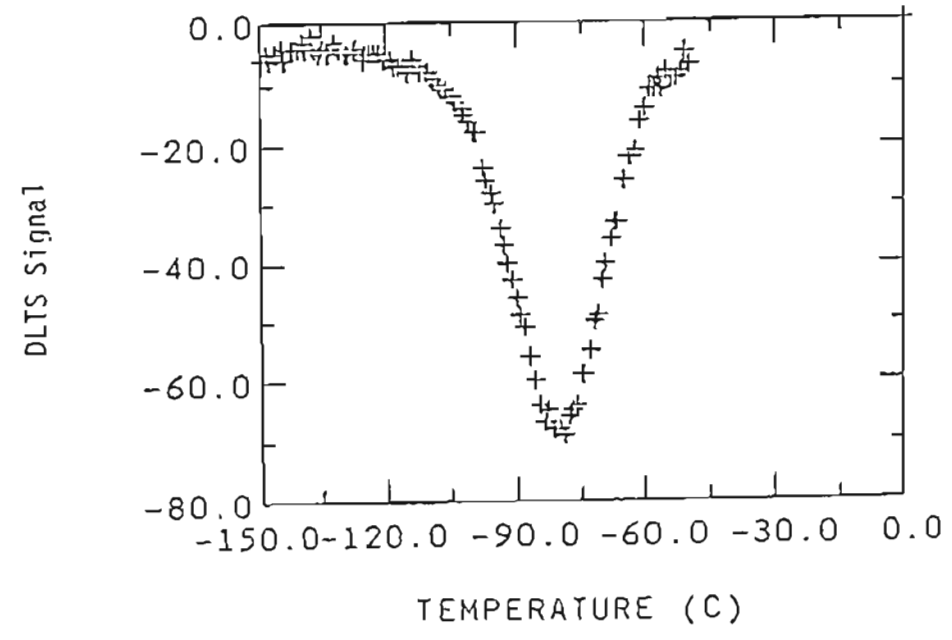

FIG. 17B. DLTS plot of InP-23.

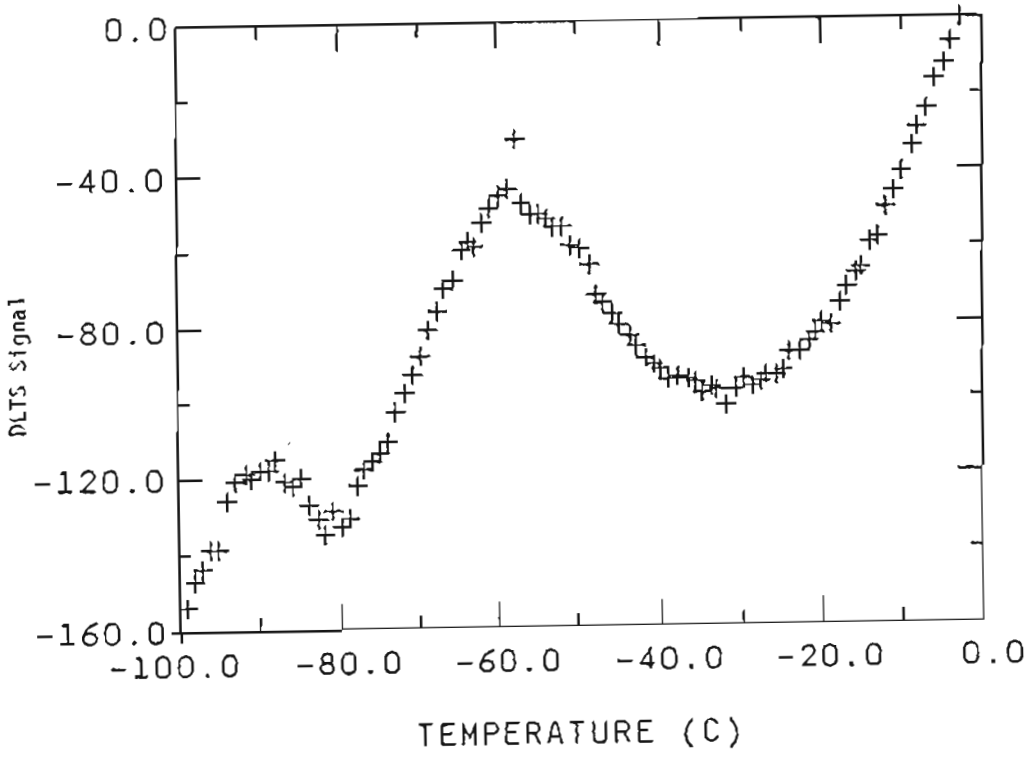

FIG. 17C. DLTS plot of InP-59

temperature (-80^{0}C) and hence represent the same trap as shown in Fig. (17 A-C). As this trap is observed in four out of five samples tesed,it is believed to be an inherent defect and not an accidental contaminant. The Arrhenius plot of all these samples are combined and a straight line is fitted to selected data points, using the least-square method. Fig. (18) represents this plot from which the activation energy and capture cross section are calculated to be 0.31 eV and $3.17 \times 10^{-17} cm^2$ respectively. This trap will be refered to as H(0.31). The summary of DLTS parameters is given in Table IV. It should be noted that the trap concentration of H(0.31) in Fig. (17 C) is very low (1 part in 10^{10}) and there is a lot of noise which makes it difficult to observe. The resistivity of the sample is high as the dopant density is low and hence trap re-filling becomes difficult. In spite of all these problems, a fairly well-behaved Arrhenius plot is obtained for this trap.

Figure (19) shows the log-log plot of Cp_2Mg/TMIn Vs. trap concentration of H(0.31). Increase in Mg/In ratio does show some apparent change in concentration of H(0.31), however it is weak and hence does not represent a DX center, where a much stronger dependence on free carrier density is usually observed. The traps H(0.54) at -35^{0}C

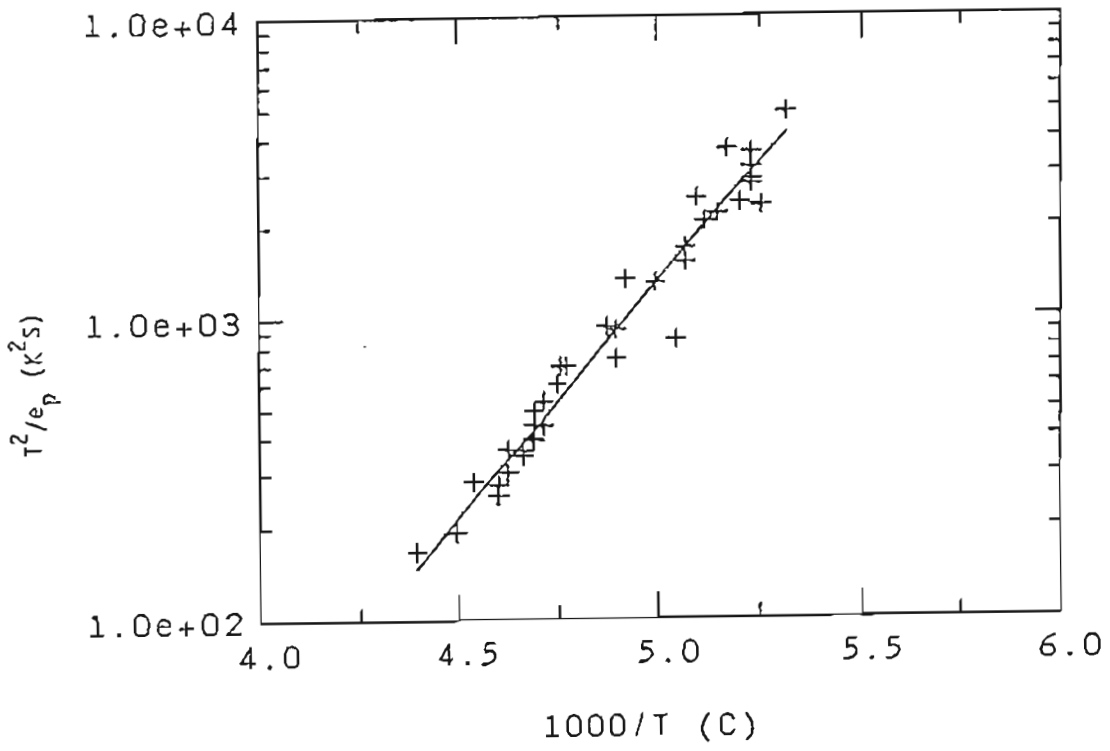

FIG. 18. Arrhenius plot of trap level H(0.31).

TABLE IV. Summary of DLTS parameters.

Sample Number	N_A (Cm^{-3})	Trap Label	Activation Energy E_A (eV)	Capture Cross section σ_p(Cm^2)	Trap Concentration N_T(Cm^{-3})
InP 20	4.19×10^{15}	H(0.31)	0.31	3.17×10^{-17}	$3\text{-}6\times10^{13}$
InP 23	7.32×10^{15}	H(0.31)	0.31	3.1710^{-17}	$2\text{-}8\times10^{14}$
InP 57	5.62×10^{13}	H(0.31)	0.31	3.17×10^{-17}	$6\times10^{13}\text{-}2\times10^{14}$
InP 59	2.09×10^{12}	H(0.31)	0.31	3.17×10^{-17}	$1\text{-}3\times10^{12}$
		H(0.54)	0.54	1.52×10^{-14}	$1\text{-}4\times10^{12}$
InP 61	5.97×10^{14}	H(1.16)	1.16	2.7×10^{-7}	$5\times10^{13}\text{-}2\times10^{14}$

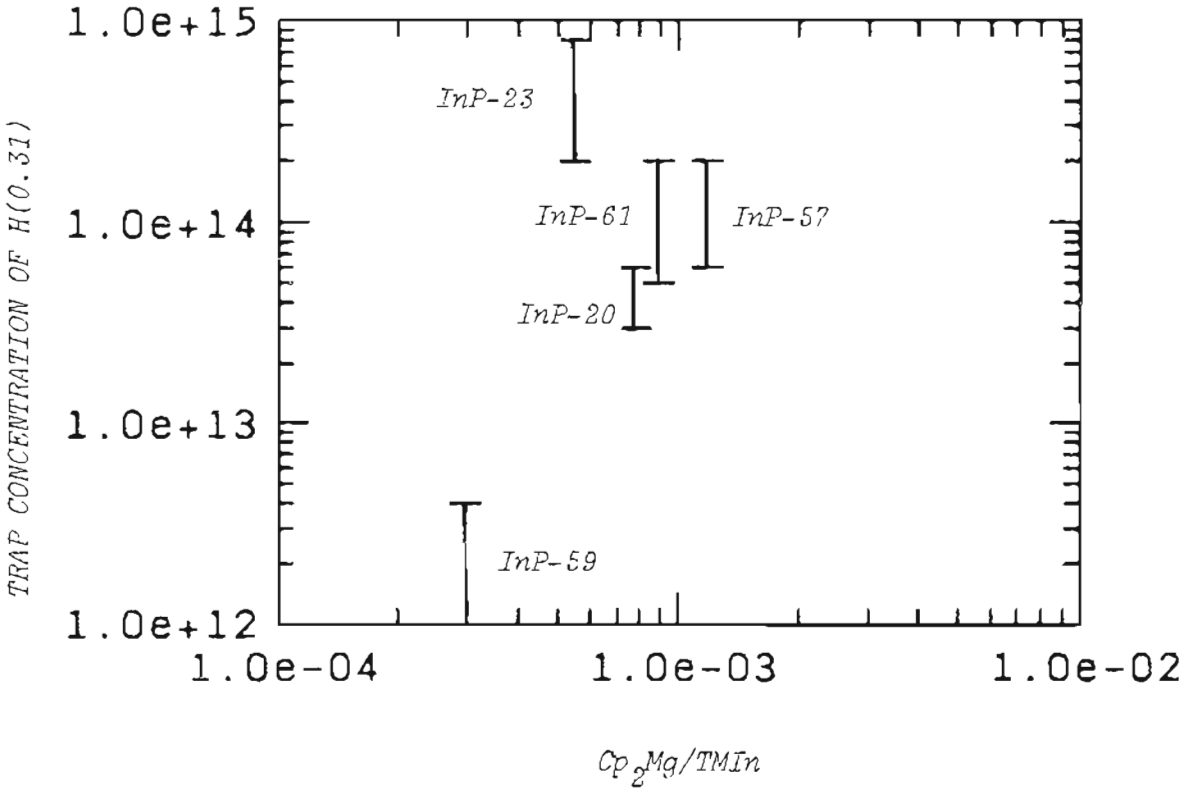

FIG. 19. Cp_2Mg/TMIn Vs. Trap Concentration of H(0.31).

and H(1.16) at 40^0C observed in this study are not found in all the samples and are probably due to contaminants. H(1.16) occured above room temperature and as $100-350^0$K is a typical temperature range for emission of carriers from interface states, this was verifiedas follows (68). First the pulse voltage (ΔV) was maintained at 1V, while the quiescent reverse bias (V_R) was changed. The presence of interface states would shift the peak of the DLTS spectrum to lower temperatures. Next, V_R was kept constant and ΔV was altered. Here the presence of interface states would increases the peak height. Neither of these effects were observed in H(1.16). Hence it is concluded that the defect in InP-61 was bulk and not due to interface defects.

Before coming to a conclusion about the physical identity of the trap H(0.31), it is compared with the traps reported in the p-InP literature. For instance, a trap with activation energy 0.22 eV has been observed by DLTS in both LPE and VPE grown InP:Zn (38, 40). This defect has been identified as impurity-phosphorous vacancy complex in the LPE grown material and as a residual impurity in the VPE grown material. This trap has been seen in the temperature range $120-273^0$K, which is close to the range in which H(0.31) was observed. The capture cross section of H(0.22)

measured by J. L. Pelloie et. al. is $0.1x10^{-16}cm^2$ (38) and that reported by Inuishi is $0.04x10^{-16}cm^2$ (40). In addition to H(0.22), Inuishi has found H(0.29), H(0.40) and H(0.50) in VPE grown InP with capture cross sections of $4x10^{-16}$, $4x10^{-16}cm^2$ and $3x10^{-16}cm^2$ respectively. He has identified these traps also as residual impurities. Since many more traps are observed in the VPE material as compared to the OMVPE material of this study, it is believed that H(0.31) is not a residual impurity, but is either an isolated native defect or a Mg-native defect complex. To determine whether the trap is an isolated defect or a magnesium-related complex, the results are compared with those reported in the literature. If the trap is found in all p-type InP samples listed in Table I, regardless of the type of dopants and the growth methods used, the trap is an isolated native defect. If, however, the defect is unique to the OMVPE InP, it is related to the dopant used. It is seen that H(0.31) is quite different from the traps observed in the past and hence it cannot be an isolated defect. H(0.21) has been found in Vanadium-doped InP codoped with Zn using PL, DLTS, DLOS and absorption experiments (34, 35, 36). This defect has been identified as vanadium-related defect. Hence H(0.31) is ascribed to Mg-related defect.

CHAPTER 6

CONCLUSIONS

Defects in Mg-doped InP grown by OMVPE have been investigated using DLTS. This characterization technique has been found to be very versatile in providing information about the trap parameters like the activation energy, capture cross section, density and nature of the trap.

The electronic properties of these InP epitaxial layers were studied using CV and IV measurements. The net carrier concentration, barrier height and ideality factor were calculated from these measurements. The net acceptor concentration was in the range of 10^{12} to 10^{15} cm^{-3}, the barrier height was measured to be 0.75 eV from CV analysis and about 0.49 from IV measurements for one of these samples. The ideality factor was about 3.1.

The DLTS measurements revealed three hole traps with activation energies of 0.31, 0.54 and 1.16eV. The capture cross sections of these traps were calculated to be $1.7x10^{-16}$, $1.5x10^{-14}$ and $2.7x10^{-7}$ cm^2 respectively.

The trap concentration ranged from 10^{12}-10^{15} cm^{-3}.

These trap characteristis were compared to that reported in the literature on p-type InP, and the physical identity of the traps observed in this work are speculated. The trap H(0.31) is ascribed to a Mg-related complex and H(0.54) and H(1.16) are thought to be caused by contaminants.

REFERENCES

1. D. V. Lang, "Deep Level Transient Spectroscopy: A new method to characterize traps in semiconductors", J. Appl. Phys., 45, No.7, 3023 (1974)

2. J. Criado, A. Gomez, E. Munoz and E. Calleja, "Deep Level Transient Spectroscopy signature analysis of DX centers in AlGaAs and GaAsP", Appl. Phys. Lett., 49 (26), 1790 (1986)

3. D. V. Lang, Deep centers in semiconductors, Edited by Pantelides, 489 (Gordon and Breach, New York, 1985)

4. K. J. Bachmann, "Properties, preparation and device application of InP", Ann. Rev. Mater. Sci., 441 (1981)

5. H. Morkoc, J. Andrews, S. B. Hyder and S. G. Bandy, "InP MESFETS prepared by VPE", Inst. Phys. Conf. Ser., 45, 295 (1979)

6. L. Messick, "Power gain and noise of InP and GaAs Insulated Gate Microwave FETS", Solid-State Electronics, 22, 71 (1978)

7. H. H. Wieder, "Problems and prospects of compound semiconductor field effect transistors", J. Vac. Sci. Technol., 17(5), 1009 (1980)

8. P. D. Wright, Y. G. Chai and G. A. Antypas, "InGaPAs-InP Double - Hetrojunction High-Radiance LED's", IEEE Trans. of Elect. Devices, ED-26, No. 8, 1220 (1979)

9. H. Nishi, M.Yano, Y.Nishitani, Y.Akita and M. Takusagawa, "Self-aligned structure InGaAsP/InP DH lasers", Appl. Phys. Lett., 35(3), 232 (1979)

10. J. S. Escher, R. L. Bell, P. E. Gregory, S. B. Hyder, T. J. Maloney, and G. A. Antypas, "Field-Assisted Semiconductor Photoemitters for the 1-2μ range", IEEE Trans. of Elect. Devices, ED-27, No.7, 1244 (1980)

11. A. W. Nelson and L. D. Westbrook, "A study of p-type dopants for InP grown by Adduct MOVPE", J. Cryst. Growth, (68), 102 (1984)

12. F. Capasso, K. Mohammed and A. Y. Cho, " Tunable

barrier heights and band discontinuities via doping interface dipoles. An interface engineering technique and its device applications", J. Vac. Sci. Technol., B3, 1245 (1985)

13. F. R. Bacher and W. B. Leigh, "Photoluminescence study of Mg doped MOVPE InP", J. Cryst. Growth, 80, 456 (1987)
14. F. A. Kroger, The chemistry of imperfect crystals, vol. 1, 2, 3, second edition, (Interscience, New-York, 1964)

15. G. L. Miller, D. V. Lang and L. C. Kimerling, "Capacitance transient spectroscopy", Ann. Rev. Mater. Sci., 377 (1977)

16. P. J. Dean, "PL as a diagnostic of semiconductors", Proc. Cryst. Growth. Charact., 5, 89-174 (1982)

17. T. S. Moss, Optical properties of semiconductors, (Acadamic, New-York, 1959)

18. L. J. Van der Pauw, "A method of measuring specific resistivity and hall effect of dics of arbitrary shape", Philips Res. Rep., 13, 1 (1958)

19. R. E. Kremer, M. C. Arikan, J. C. Abele and J. S. Blakemore, "Transient photoconductivity measurements in semi-insulating GaAs. An analog approach", J. Appl. Phys., 62(6), 2424 (1987)

20. J. C. Abele, R. E. Kremer and J. S. Blakemore, "Transient photoconductivity measurements in SI GaAs. A digital approach", J. Appl. Phys., 62(6), 2432 (1987)

21. D. V. Lang, "Fast capacitance transient apparatus: Application to ZnO and O centers in GaP p-n junction", J. Appl. Phys., 45, No. 7, 3014 (1974)

22. W. B. Leigh and R. E. Kremer, "Deep level defects in CdTe", Mat. Res. Soc. Symp. Proc., 90, 241 (1987)

23. M. Levinson, J. L. Benton, H. Temkin, and L. C. Kimerling, "Defect states in electron bombarded n-InP", Appl. Phys. Lett., 40(11), 990 (1982)

24. J. Suski, A. Sibille and J. Bourgoin, "Defects in low temperature electron irradiated InP", Solid State. Comm., 49, 875 (1984)

25. A. Sibille, J. Suski and G. Le Roux, "Energy and orientation dependence of electron-irradiation-induced defects in InP", Phys. Rev., B30, 119 (1984)

26. A. Sibille and E. V. K. Rao, "Electron irradiation defects in InP", J. Crys. Growth, 64, 194 (1983)

27. A. Sibille and J.C. Bourgoin, "Electron irradiation induced deep levels in p-InP", Appl. Phys. Lett., 41(10), 956 (1982)

28. M. Levinson, H. Temkin, and W. A. Bonner, "Electron bombardment induced defect states in p-InP", J. Elec. Mater., 12, 423 (1983)

29. A. Sibille, " Electric Field Effects on radiation defects annealing in p-InP", Solid States. Comm., 46(9), 673-675 (1953)

30. A. Sibille, "Thermal and injection enhanced annealing of electron irradiation induced defects in InP", 13th Int. conf. on defects in semiconductors, 1155-1162 (1984)

31. L. A. Hemstreet, "The electronic states of 3D transition metal impurities in InP", 13th Int. conf. on defects in semiconductors, 1043-1049 (1984)

32. A. Sibbile, E. V. K. Rao and A. Mircea, "Transition metal impurities in InP: Defect complexes and native defects", Proc. of 16th int. conf. on phy. of semicond. part-1, Montpellier, France, 176 (1982)

33. B. Clerjaud and C. Naud, "The acceptor level of vanadium in III-V compounds", J. Appl. Phys., 58(11), 4207 (1985)

34. Georges Bremond, A. Nouailhat, G. Guillot, B. Daveaud, B. Lambert, Y. Tondic, B. Clerjaud and C. Naud, "The donor state of vanadium in InP", Microscopic identification of elctronic defects in semicond., Mat. Res. Soc. Symp. Proc., 46, 359 (1985)

35. B. Devaud, B. Plot and B. Lambert, "The donor level of vanadium in InP", J. Appl. Phys., 59(9), 3126 (1986)

36. B. Clerjaud, D. Cote, C. Naud, G. Bremond, G. Guillot and A. Nouailhat, "Spectroscopic investigation of vanadium in InP", J. Cryst. Growth, 83, 194 (1987)

37. C. D. Brandt, A. M. Hennel, L. M. Pantowicz, Y. T. Wu, T. Bryskiewicz, J. Lagowski and H. C. Gatos, "New semi-insulating InP: Titanium midgap donors", Appl. Phys. Lett., 48(17), 162, (1986)

38. J. L. Pelloie, G. Guillot and N. Nouailhat and A. G. Antolini, "A study of deep levels by transient spectroscopy on p-type LPE $Ga_xIn_{1-x}As_yP_{1-y}$ grown on SI InP", J. Appl. Phys., 59(5), 1536 (1986)

39. B. Clerjaud, D. Cote and C. Naud, "Evidence for Hydrogen-Transition-Metal Complexes in As-grown InP", J. Cryst. Growth, 83, 190 (1987)

40. M. Inuishi and B. W. Wessels, "Deep hole traps in VPE p-type InP", Elec. Lett., 17, No. 19, 685 (1981)

41. S. S. Li, W. L. Wang and E. H. Shaban, "Characterization of the grown-in defects in Zn-doped InP", Solid Stat. Comm., 51, 15, No. 1, (1984)

42. E. V. K. Rao, M. Djamei and M. Duhamel, "Defect-impurity interactions in Zn implanted SI InP", 13th int. conf. on defects in semiconductors, 1123-1131 (1984)

43. J. M. Kuo and F. A. Thiel, "Study of deep level in bulk p-InP by admittance spectroscopy", Elec. Lett., 19, No.2, 41 (1983)

44. S. H. Chiao and G. A. Antypas, "Photocapacitance effects of deep traps in n-type InP", J. Appl. Phys., 49(1), 466 (1978)

45. A. M. White, A. J. Grant and B. Day, "Deep traps in ideal n-InP Schottky diode", Elec. Lett., 14(13), 409 (1978)

46. A. Majerfeld, O. Wada and A. N. M. M. Choudhury, "Deep level traps and the conduction-band structure of InP", Appl. Phys. Lett., 33(11), 957 (1978)

47. S. R. McAfee, F. Capasso, D. V. Lang, A. Hutchinson, and W. A. Bonner, " A study of deep level in bulk n-InP by transient spectroscopy", J. Appl. Phys., 52(10), 6158 (1981)

48. M. Levinson, J. L. Benton and L. C. Kimerling, "Electronically controlled metastable defect reactions in InP", Phys. Rev. B. 27, No. 10, 6216 (1983)

49. M. Levinson, M. Stavola, J. L. Benton and L. C. Kimerling, "Metastable M center in InP: Defect-charge-state-controlled structural relaxation", Phy. Rev. B. 28, No. 10, 5848 (1983)

50. M. Stavola, M. Levinson, J. L. Benton and L. C. Kimerling, "Extrinsic self-trapping and negative u in semiconductor: A metastable center in InP", Phy. Rev. B. 30, No. 2, 832 (1984)

51. M. Stavola, M. Levinson, J. L. Benton and L. C. Kimerling, "Large Lattice relaxation in a multielectron system-binding energies and criteria for negative effective u", 13th int. conf. on defects in semiconductors, 191, (1984)

52. M. Levinson and M. Stavola, "Configurationally bistable MFe center in InP", 13th int. conf. on defects in semiconductors, 1133 (1987)

53. J .F. Wager and J. A. Van Vechten, "Identification of M centers in InP", Mat. Res. Soc. Symp. Proc. 46 325 (1985)

54. M. Levinson, "Capcitance transient analysis of configurationally bistable defects in semiconductors", J. Appl. Phys., 58(7), 2628 (1985)

55. T. A. Kennedy and N. D. Wilsey, "Electron paramagnetic resonance identification of the phosphorous antisite in electron irradiated InP", Appl. Phys. Lett., 44(11), 1089 (1984)

56. N. D. Wilsey and T. A. Kennedy, "Electron paramagnetic resonance of intrinsic defects in III-V semiconductors", Mat. Res. Soc. Symp. Proc., 46, 309 (1985)

57. J. Shirafuji, J. Koyama, and Y. Inuishi, "Gamma-ray induced defects and their annealing behavior in n-InP", 13th int. conf. on defects in semiconductors, 1149-1154, (1984)

58. F. R. Bacher, "OMVPE growth and characterization of InGaAs and InP". Ph.D. Thesis, Oregon Graduate Center, (1987).

59. F. R. Bacher, H. Cholan, and W. B. Leigh, "Defects in Mg-doped InP and GaInAs grown by OMVPE", Mat. Res. Soc. Symp. Proc., 90 (1987)

60. S. M. Sze, Physics of semiconductors, second edition (John Wiley & Sons, 1981)

61. A. Mitonneau, G. M. Martin and A. Mircea, " Electron traps in bulk and epitaxial GaAs crystals", Electron. Letters, 13, No. 22 191 (1977)

62. G. Vincent, A Chantre and D. Bois, "Electric field effects on thermal emission of traps in semiconductor junctions", J. Appl. Phys. 50, 5484 (1979)

63. D. V. Morgan, J. Frey and W. J. Devlin, "Rectifying and ohmic contacts to GaInAsP", J. Electrochem. Soc., 125, No. 5, 1202 (1980)

64. J. D. Wiley and G. L. Miller, "Series resistance effects in semiconductor CV profiling", IEEE Trans. on Electron Devices, ED22, No. 5, 265 (1975)

65. Inuishi, Masahide, "Determination of bulk states and interface states in vapor grown InP using transient capacitance spectroscopy", Ph.D. Thesis, Northwestern University (1982)

66. Edward J. Bawolek, M.S. Thesis, Northwestern University (1982)

67. C. T. Sah, L. Forbes, L.. L. Rosier and A. F. Tasch, Sold State Elect. 13, 759 (1970)

68. F. Murray, R. Carin and P. Bogdanski, "Determination of high-density interface state parameters in metal-insulator-semiconductor structures by Deep Level Transient Spectroscopy", J. Appl. Phys., 60(10), 3592 (1986)

VITA

The author was born 22nd May 1963, in Calcutta, India. In 1970 she moved to Madras and graduated from high school in 1980. She then began study at College of Engineering, Anna University, Madras, where she received her Bachelor of Science degree in May 1983.

In December 1983 the author was married to Cholan Muthukumarasamy and then moved to United States in January 1985.

She began her studies in April 1985 at Oregon Graduate Center. Doing her thesis work under the direction of Dr. Wallace B. Leigh, the requirements for a Master of Science degree in Electrical Engineering were completed in December 1987.